RIGA TECHNICAL UNIVERSITY

Natālija Bulaha

APPLICATION OF 3D AND 2D SURFACE ROUGHNESS PARAMETERS IN CONTACT AND WEAR RESISTANCE EVALUATION

Summary of the Doctoral Thesis

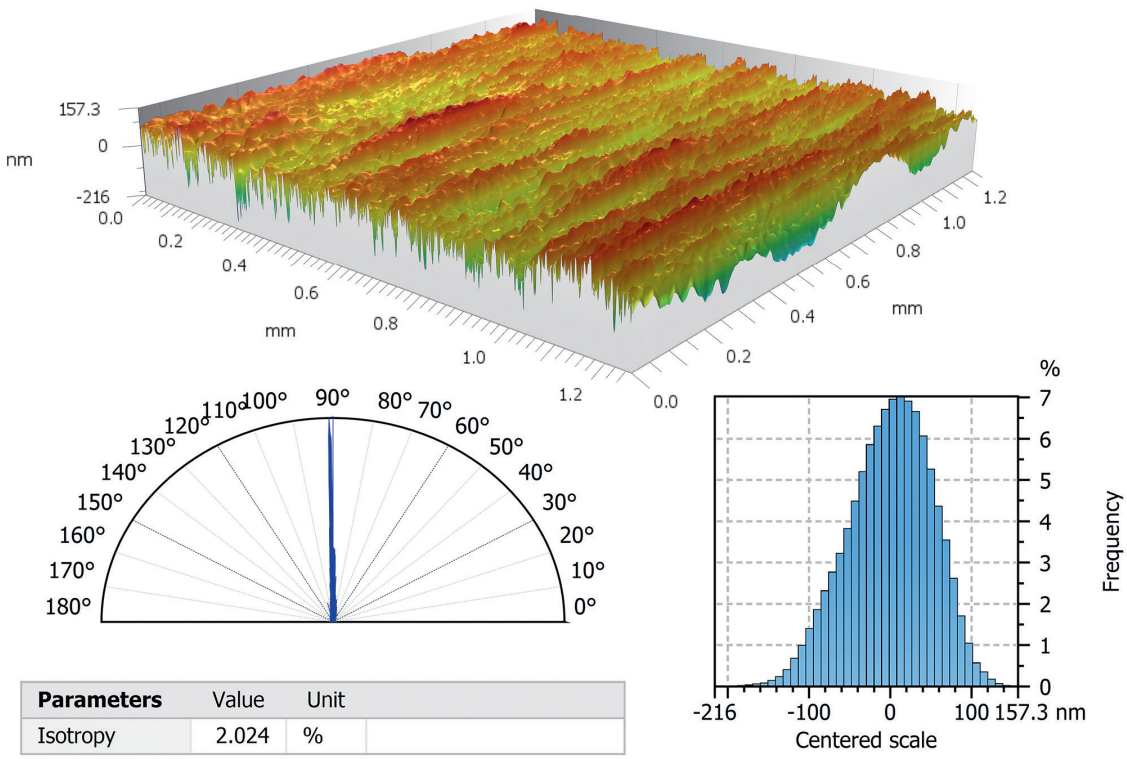

Parameters	Value	Unit	
Isotropy	2.024	%	

RTU Press
Riga 2026

RIGA TECHNICAL UNIVERSITY
Faculty of Civil and Mechanical Engineering
Institute of Mechanical and Biomedical Engineering

Natālija Bulaha
Doctoral Student of the Study Programme "Mechanical Engineering and Mechanics"

APPLICATION OF 3D AND 2D SURFACE ROUGHNESS PARAMETERS IN CONTACT AND WEAR RESISTANCE EVALUATION

Summary of the Doctoral Thesis

Scientific supervisors

Professor Dr. sc. ing.
OSKARS LINIŅŠ

Docent Dr. sc. ing.
ANITA AVIŠĀNE

Professor Dr. habil. sc. ing.
JĀNIS RUDZĪTIS

RTU Press
Riga 2026

Bulaha, N. Application of 3D and 2D Surface Roughness Parameters in Contact and Wear Resistance Evaluation. Summary of the Doctoral Thesis. Riga: RTU Press, 2026. 52 p.

Published in accordance with the decision of the Promotion Council "RTU P-04" of 16 October 2025, Minutes No.04030-9.4/3.

The Doctoral Thesis was partly developed within the project "VPP-IZM-Sports-2023/1-0001 Innovations, methodologies and recommendations for the development and management of the sports sector in Latvia".

The author expresses gratitude to Mitutoyo Poland for providing access to the Mitutoyo Formtracer avant S-3000 measurement machine and the MCubeMap Ultimate 10 software, which were necessary for the completion of this study.

Cover picture by Natālija Bulaha.

https://doi.org/10.7250/9789934372551

ISBN 978-9934-37-255-1 (pdf)

DOCTORAL THESIS PROPOSED TO RIGA TECHNICAL UNIVERSITY FOR PROMOTION TO THE SCIENTIFIC DEGREE OF DOCTOR OF SCIENCE

To be granted the scientific degree of Doctor of Science (PhD), the present Doctoral Thesis has been submitted for defence at the open meeting of RTU Promotion Council on February 4, 2026 at 14.30 at the Faculty of Civil and Mechanical Engineering of Riga Technical University, 6B Ķīpsalas Street, Room 417.

OFFICIAL REVIEWERS

Leading researcher *Dr. sc. ing.* Ernests Jansons,
Riga Technical University

Assistant professor *Dr. eng.* Daniel Grochala,
West Pomeranian University of technology Szczecin, Poland

Professor *Dr.* Juozas Padguskas,
Vytautas Magnus University, Lithuania

DECLARATION OF ACADEMIC INTEGRITY

I hereby declare that the Doctoral Thesis submitted for review to Riga Technical University for promotion to the scientific degree of Doctor of Engineering Sciences is my own. I confirm that this Doctoral Thesis has not been submitted to any other university for promotion to a scientific degree.

Natālija Bulaha ……. (signature)
Date: ……

The Doctoral Thesis has been written in Latvian. It consists of an Introduction, 5 chapters, Conclusions, 65 figures, 22 tables, and 1 appendix; the total number of pages is 114, including appendix. The Bibliography contains 81 titles.

TABLE OF CONTENTS

GENERAL CHARACTERISTICS OF THE DOCTORAL THESIS

Actuality of the topic

The issue of ensuring the wear resistance of friction pair surfaces always remains relevant. The ability to control and predict wear allows us to optimize several processes: 1) part manufacturing – choice of suitable materials and processing modes to obtain a product with the required mechanical properties and quality; 2) lubrication procedures; 3) operating parameters – load, speed, temperature, to extend the normal exploitational period. Also important is the planning of technical maintenance, with the help of which you can reduce downtime and maximize the service life of components.

As is known, the wear intensity of parts is influenced by several factors: the material and its properties, environmental conditions, lubrication, load, pressure, and the quality of the surface, which has particular importance in this matter, since the type of processing and roughness parameters largely determine the operational properties and service life of the surface. In friction pairs of machine components, surfaces treated with abrasive tools are mainly used, which provide the necessary surface smoothness and accuracy. Surfaces, after such treatment, are characterized by an irregular arrangement of micro-irregularities and a pronounced direction of the machining traces. In turn, such texture features make it difficult to accurately determine the roughness parameters both in an analytical way and using computer processing programs. First, this is due to the deviation of the ordinate distribution from the normal distribution law, as well as the features of the roughness profile parallel to the processing traces, which do not allow to accurately determine the roughness step in the friction direction. An important role is played by computer processing of the surface texture, which greatly affects the surface geometry and roughness parameter values.

Existing wear calculation models include 2D roughness parameters, the correctness of the application of which and the accuracy of determination are not justified, which reduces the reliability of the obtained results. To correctly and accurately determine and predict the wear of friction pair surfaces, it is necessary to create an improved wear determination model with correctly determined roughness parameters. For this purpose, the following goals and corresponding tasks were formulated.

Aim and tasks of the work

The aim of the doctoral thesis

To develop a specified calculation model for wear and a linear wear intensity for a sliding friction pair, based on the theory of material fatigue, and ensure the accuracy of the determination of the roughness parameters included in this model.

Tasks

1. Research and analysis of information sources.
2. Experimental determination of 2D and 3D surface roughness.
3. Selection of a leveling operation for determining the surface geometry and the mean plane.
4. Verification of the mathematical model of a 3D surface with irregular roughness.

5. Verification of the accuracy of the determination of the 3D and 2D roughness parameters.
6. Development of a calculation model for linear wear and wear intensity.

Research methods

1. Experimental determination of 2D and 3D surface roughness was carried out by the contact method (stylus – the surface under study) with a profilometer Mitutoyo Formtracer avant S-3000.
2. Processing of experimental results was carried out in the computer processing program McubeMapUltimate 10.
3. Leveling of the surface texture was carried out by the least squares method, the minimum zone method and mean subtraction.
4. The compliance of the surface ordinate distribution function with the normal distribution law was checked by the 3rd and 4th moments of the normal random function.
5. Random functions/field theory was used to mathematically express the 3D roughness parameters of irregular surfaces.
6. Robust Gaussian filtration was used to determine the surface roughness step in a direction parallel to the processing traces.
7. Calculations of the linear wear and wear intensity of the friction pair of parts were based on the theory of material fatigue.
8. The Excel program was used for the calculation part, comparison of results and construction of graphs.

Scientific novelty

1. A new model for the calculation of wear and wear intensity, which includes 3D and 2D roughness parameters of the contact surface and material fatigue characteristics for elastic and plastic contact cases.
2. A new approach for ensuring the accuracy of roughness parameters:

2.1. Application of leveling operations and correction coefficient for the determination of the roughness step RSm_2 at the standardized evaluation length.

2.2. Inclusion of the kurtosis value of the roughness ordinate distribution function in the calculations of the arithmetic mean height *Sa*.

2.3. Evaluation of surface roughness anisotropy using the 3D roughness parameter *Str* – surface texture aspect ratio of the standard ISO 25178-2.

2.4. Determination of the volume of deformed material using the standard ISO 25178-2 3D roughness parameter *Vm* – material volume.

Practical application

1. A new wear and wear intensity calculation model can be adapted to the finite element environment to determine and predict the wear of friction pair surfaces for a specific number of cycles.
2. The formulas for roughness parameter calculation can be used to control roughness parameters in the finite element environment during the surface wear simulation period.
3. The obtained relationships can be used in studies of real friction components.

Approbation of obtained results

International scientific conferences

1. 24th International Scientific Conference **Engineering for Rral Development, 2025.**
   Report *"Influence of various factors on the determination accuracy of surface profile elements for engineering calculations"*.
2. 16th International Scientific Conference **Engineering for Rural Development, 2017.**
   Report *"Analysis of Model and Anisotropy of Surface with Irregular Roughness"*.
3. **RTU 58th** International Scientific Conference, 2017.
   Report *"Application of 3D roughness parameters for engineering tasks solution"*.
4. 15th International Scientific Conference **Engineering for Rural Development, 2016.**
   Report *"Measurement Principles of 3D Roughness Parameters"*.
5. **RTU 57th** International Scientific Conference, 2016.
   Report *"Determination of roughness average steps for surfaces with irregular character"*.
6. **RTU 56th** International Scientific Conference, 2015.
   Report *"Analysis of honed and lapped surfaces roughness structure and 3d parameters"*.
7. 14th International Scientific Conference **Engineering for rural development, 2015.**
   Report *"Surface Texture Parameters for Flat Grinded Surfaces"*.
8. 10th International Scientific Conference **Environment. Technology. Resources.**
   Report *"Analysis of Service Properties of Cylindrically Ground Surfaces, Using Standard ISO 25178-2:2012 Surface Texture Parameters"*.
9. **RTU 55th** International Scientific Conference, 2014.
   Report *"The Measurement of Surface Texture for Nanostructured Coatings"*.
10. 8th International Scientific Conference **Materials, Environment, Technology, MET-2013.**
    Report *"Analysis of standardization development of surface roughness parameters"*.

Publications

1. Bulaha, N. Influence of various factors on the determination accuracy of surface profile elements for engineering calculations. In: 24th International Scientific Conference "Engineering for Rural Development" Proceedings. Vol. 24, 2025, pp. 519–531 (SCOPUS).
2. Bulaha, N., Liniņš, O., Avišāne, A. Application of 3D Roughness Parameters for Wear Intensity Calculations. Latvian Journal of Physics and Technical Sciences, 2021, Vol. 58, No. 5, pp. 27–37 (SCOPUS).
3. Bulaha, N., Rudzitis, J. Calculation Possibilities of 3D Parameters for Surfaces with Irregular Roughness. Latvian Journal of Physics and Technical Sciences, 2018, Vol. 55, No. 4, pp. 70–79 (SCOPUS).
4. Bulaha, N. Calculations of surface roughness 3D parameters for surfaces with irregular roughness. In: 17th International Scientific Conference "Engineering for Rural Development" Proceedings, Vol. 17, Latvia, Jelgava, 23–25 May 2018. Jelgava, 2018, pp. 1437–1444 (SCOPUS).

5. Bulaha, N., Rudzītis, J. Analysis of Model and Anisotropy of Surface with Irregular Roughness. In: 16th International Scientific Conference “Engineering for Rural Development” Proceedings, Vol. 16, Latvia, Jelgava, 24–26 May 2017, Jelgava, 2017, pp. 1123–1130 (SCOPUS).
6. Bulaha, N., Rudzītis, J., Lungevičs, J., Liniņš, O., Krizbergs, J. Research of Surface Roughness Anisotropy. Latvian Journal of Physics and Technical Sciences, 2017, Vol. 54, No. 2, pp. 46–54 (SCOPUS).
7. Rudzītis, J., Bulaha, N., Lungevičs, J., Liniņš, O., Bērziņš, K. Theoretical Analysis of Spacing Parameters of Anisotropic 3D Surface Roughness. Latvian Journal of Physics and Technical Sciences, 2017, Vol. 54, No. 2, pp. 55–63 (SCOPUS).
8. Spriņģis, G., Rudzītis, J., Geriņš, Ē., Bulaha, N. Theoretical Approach of Wear for Slide-Friction Pairs. In: Solid State Phenomena, Poland, Bialystok, 3–8 July 2016, Trans Tech Publications, 2017, pp. 202–211 (Research Gate).
9. Bulaha, N., Lungevičs, J., Rudzītis, J. Measurement Accuracy Problems of the Surface Texture Parameters. In: 12th International Conference "Mechatronic Systems and Materials Intelligent Technical Systems": Solid State Phenomena. Volume 260, Poland, Bialystok, 3–8 July 2016. Bialystok University of Technology, 2017, pp. 227–234 (SCOPUS).
10. Bulaha, N., Rudzītis, J., Lungevičs, J., Čudinovs, V. Measurement Principles of 3D Roughness Parameters. In: 15th International Scientific Conference "Engineering for Rural Development" Proceedings, Vol. 15, Latvia, Jelgava, 25–27 May 2016. Jelgava: 2016, pp. 1059–1064 (SCOPUS).
11. Leitāns, A., Bulaha, N., Lungevičs, J. Tribological Properties of Sputter Deposited Carbon-Copper Composite Films. In: Proceedings of VIII International Scientific Conference BALTTRIB' 2015, Lithuania, Kaunas, 26–27 November 2015. Kaunas, Aleksandras Stulginskis University, 2016, pp. 61–65 (SCOPUS).
12. Bulaha, N., Rudzītis, J. Surface Texture Parameters for Flat Grinded Surfaces. In: 14th International Scientific Conference "Engineering for Rural Development" Proceedings, Vol. 14, Latvia, Jelgava, 21–22 May 2015. Jelgava, Latvia University of Agriculture, 2015, pp. 810–816 (SCOPUS).
13. Bulaha, N. Analysis of Service Properties of Cylindrically Ground Surfaces, Using Standard ISO 25178-2:2012 Surface Texture Parameters. In: Environment. Technology. Resources, Proceedings of the 10th International Scientific and Practical Conference, Vol. 1, Latvia, Rezekne, 18–20 June 2015, Rezeknes University, 2015, pp. 16–21 (SCOPUS).

GLOSSARY

Ssk – skewness of surface ordinates distribution;
Sku – kurtosis of surface ordinates distribution;
Sq – surface root mean square height, μm;
Sa – surface arithmetic mean height, μm;
Str – surface texture aspect ratio;
Sz – surface maximum height, μm;
$Smr(c)$ – areal material ratio, mm^2;
Vm – material volume, mm^3;
c – surface level, μm;
γ – relative deformation level;
$\Phi()$ – Laplace transform;
Xs – mean width of profile elements, mm;
RSm_1 – mean roughness profile element spacing in X-axis direction, mm;
RSm_2 – mean roughness profile element spacing in Y-axis direction, mm;
WSm – mean waviness profile element spacing in Y-axis direction, mm;
Ra – profile arithmetic mean height, μm;
Rsk – skewness of profile ordinates distribution;
Rku – kurtosis of profile ordinates distribution;
Rq – profile root mean square height, μm;
Rp – mean profile peak height, μm;
Rv – mean profile pit depth, μm;
C – coefficient of anisotropy;
Aa – evaluation area (nominal area), mm^2;
$N(0)$ – number of profile intersections with the mean line;
$n(0)$ – number of zeros per unit length, mm^{-1};
k_{pr} – correction coefficient;
$f_{ACF}(t_x,t_y)$ – autocorrelation function;
S_{al} – autocorrelation length, mm;
R – radius of autocorrelation function, mm;
s – level of the autocorrelation function section;
$E\{\}$ – expected value;
$D\{\}$ – dispersion;
L – evaluation length, mm;
l – section length, mm;
$LSPL$ – least square plane leveling;
$TLSPL$ – total least square plane leveling;
$MZPL$ – minimum zone plane leveling;
PL – polynomial;
RMS_{vid} – root mean square deviation, μm;

h_{x_max}, – maximum deviation of the X-axis profile mean line from the mean plane, μm;
h_{y_max} – maximum deviation of the Y-axis profile mean line from the mean plane, μm;
n_{Sa} – number of measurement experiments;
t_β – tabulated value, depending on the confidence level β;
ε – relative error of the parameter, %;
α – correlation function approximation parameter;
Jh – linear wear intensity;
V' – volume of deformed material, mm^3;
h – linear wear depth, μm;
n – number of cycles to failure;
d – contact length, mm;
KK – contact type criterion;
θ – elastic constant of the material, MPa^{-1};
θ_{sum} – total elastic constant of material, MPa^{-1};
μ – Poisson's ratio;
E – elastic modulus, MPa;
H – hardness, MPa;
σ_0, e_0 – extrapolated values of the fatigue curve;
t_{el}, t_{plast} – fatigue curve parameters;
q_{el}, q_{plast} – load, MPa;
k_{el}, k_{plast} – coefficients that depend on the anisotropy of the surface;
σ_T – material yield strength, MPa;
L_{ber} – friction path, mm;
f – coefficient of friction;
V – rotation speed, m/s;
t – working time, s.

1. LITERATURE REVIEW

1.1. Application of surface roughness parameters in wear calculations of friction surfaces

The issues of provision of wear resistance are relevant in all areas of mechanical engineering. Calculations of wear intensity make it possible to determine the relationships between wear and material properties, surface roughness, environmental conditions and operating parameters. Basically, there are three main methods of wear determination: analytical, experimental and numerical simulation.

The analytical method includes models for wear calculation. Thus, in the 18th century, **Amonton** and **Coulomb** invented the three main basic laws of tribology, based on which the geometric model of friction was created [1]. Tribologist **Desanguliers** had proposed the concept of adhesion friction at that time [2]. He considered that adhesion was one of the processes that takes place during friction, but this contradicted experiments. **In 1950**, Desanguliers' concept of adhesive friction was further developed, as it was successfully used by **Bowden** and **Tabor** in the studies of metal-to-metal contact [3]. Bowden and Tabor showed that the static friction force between two sliding surfaces is strongly dependent on the real contact area, which was expressed as the ratio of the normal load to the hardness of the softer material.

In 1953, Archard developed a wear prediction model, which was also based on the adhesive wear mechanism [4]. Archard's model states that in the case of plastic contact, the amount of material worn Vv is directly proportional to the load F, the sliding distance s_R and the wear coefficient k, and inversely proportional to the material hardness H:

$$V_v = \frac{k}{H} \times F \times s_R \tag{1.1}$$

In 1958, Rabinowicz proposed a wear prediction model that included surface energy effects [5]. His theory establishes a link between the friction coefficient and the surface energies of solids. **In 1968, Kragelsky** formulated an opposite condition for low wear to Archard's model – the principle of a positive gradient of mechanical properties [6]. This means that the surface layers must have a lower strength than the deeper layers, otherwise catastrophic wear will occur. Kragelsky considered that friction is characterized by overcoming molecular interaction force at the points of real contact area and the resistance of the deformable material to the displacement of microirregularities by a harder body in it.

In 1980, Fleischer invented a wear determination model based on the energy approach, where the energy generated during sliding friction accumulates in the material [7]. If the accumulated energy reaches a critical limit, then the lattice energy of the material is overcome, and wear occurs. This was described by the friction energy density e_R. **In 2016, Chun,** based on the wear determination models of Rowe and Archard, included the effect of lubricants on the contact in his calculations [8]. He introduced the parameter Ψ, which characterized the ratio of the real contact area to the nominal contact area. Chun considered the deformation of surface irregularities as elastic-plastic. **In 2018, Lijesh** invented a thermodynamic approach to wear determination [9], [10]. In his works, the degradation coefficient B appears instead of the wear coefficient k, which forms a relationship between the wear rate and the entropy coefficient. However, the author does not take into account the influence of surface texture on wear.

Xiang also has a modern approach to wear determination, which includes two wear mechanisms: roughness peak deformation and fatigue mechanism [11], [12]. The author proposes to determine the amount of worn material by the fraction of wear due to plastic deformation and the proportion of fatigue cracks developing below the contact surface. In the calculations of the real contact area, the Greenwood and Williamson statistical model was used to describe rough surfaces [13], [14]. Here, it is assumed that the distribution of surface roughness ordinates corresponds to the normal distribution law to describe the contact of roughness as a function of the thickness of the lubricant film.

In 2023, Springis updated the wear calculation model of **Rudzitis** and **Konrads** based on the theory of material fatigue [15], [16], integrating into it the 3D surface roughness height parameter *Sa* [17]. The basic relationship for wear determination is similar to the expression used in the work of scientist Xiang. Springis included several factors affecting wear in the wear calculation model – surface roughness characteristics, mechanical properties, and material fatigue characteristics. However, the given model is limited by the type of contact, since it is suitable for the case of elastic contact and the Gaussian distribution of the surface ordinates.

Table 1.1 shows the main wear determination models, in which surface roughness parameters are integrated.

Table 1.1

Application of Roughness Parameters in Wear Calculation Models

#	Author	Roughness parameters
1.	Rabinowicz [5]	θ– root mean square gradient *r* – arithmetic mean peak curvature
2.	Archard [4]	*R* – arithmetic mean peak curvature
3.	Kragelsky [6]	*b, v* – parameters of material ratio curve *Rmax* – maximum height *R* – arithmetic mean peak curvature
4.	Cun [8]	*n* – density of pits β – arithmetic mean peak curvature σ – equivalent root mean square height
5.	Rudzitis [15], Konrads [16]	*Ra* – profile arithmetic mean height *c* – coefficient of anisotropy *Pc* – density of pits RSm_1 – roughness step in X-axis direction RSm_2 – roughness step in Y-axis direction
6.	Xiang [11], [12]	β – arithmetic mean peak curvature *D* – density of pits σ – root mean square height γ – texture direction
7.	Springis [17]	*Sa* – surface arithmetic mean height *Str* – surface texture aspect ratio *Pc* – density of pits RSm_1 – roughness step in X-axis direction RSm_2 – roughness step in Y-axis direction

Several wear calculation models include the wear coefficient. It is determined by performing friction experiments on a tribometer. However, to determine the wear rate

accurately, it is necessary to perform a series of experiments and statistical analysis, which requires a long time and equipment usage. In addition, the application of tribotests is limited by the testing range. Therefore, it is important to note the usefulness of the finite element method (FEM). It allows predicting surface wear mechanisms and visualizing the contact stress distribution for a specific friction pair, based on the results of tribotest measurements and an analytical wear calculation model.

Today, there are several computer programs that provide contact modeling and wear calculation, e.g., Abaqus, ANSYS, REDSY, MATHLAB, Prepromax, etc. Several wear studies include the Abaqus module UMESHMOTION, which can process changes in the geometry of contacting surfaces. Depending on the task, researchers use 2D or 3D wear simulation models. There are different options for modeling contact between two surfaces: 1) contact between two smooth surfaces; 2) contact between a rough and smooth surface; 3) contact between two rough surfaces. There are several options for generating a rough surface. Thus, the developers of the ABAQUS program in [18] and [19] offer 1) to import the 2D/3D geometry of the surface taken by the profilometer into the UMESHMOTION environment; 2) to generate a rough surface in ABAQUS with the function “Rough surface generator plug-in”; and 3) to import the rough surface generated in Matlab.

Researcher **Liang Yan’s** team performed a large-scale analysis of models for wear prediction using the FEM method [20]. Thus, most researchers, about 70 %, use the Archard model, and the second place takes the energy dissipation model, 20 %. The popularity of these models can be explained by their simplicity and fast calculation time. Other wear prediction models include electrochemical equations for corrosion wear [21], the power hardening law for thermo-mechanical wear [22], and elastic-plastic deformation models [23], which are adapted for the Archard model.

When analyzing the relevant literature, it was investigated how often researchers simulate wear processes using a rough surface contact model [24]–[35]. Thus, several scientists in their studies had simplified the surface contact model, assuming that both surfaces are smooth, i.e. roughness was not taken into account. This type of contact modeling simplifies wear calculation but affects the accuracy of the results. Most researchers note that the results of wear calculations using the Tribotest and FE methods differ, the error in some cases reaching 30 %, which can also be explained by the assumptions of the FE model. But here it is important to note both the effect of roughness on the accuracy of the model, as well as the ignoring of factors such as material fatigue, corrosion, oxidation, transverse shear stress, temperature, lubricants, etc.

1.2. Possibilities for calculating 2D and 3D surface roughness parameters

When calculating and predicting the wear of friction pair surfaces, it is important to mathematically express the roughness parameters and compare whether the experimentally determined parameter values correspond to the results of analytical calculations. This comparison will make it possible to apply analytical formulas for controlling roughness parameters during wear, which can be adapted for the finite element environment. In the Thesis, only those roughness parameters were analyzed whose precise determination is necessary in wear calculations according to the material fatigue theory.

Thus, one of the most important roughness characteristics is the parameter *Sa*, which characterizes the height properties of the surface. **Husu** and **Ruzitis** had used the random field theory for the analytical determination of the parameter *Sa* [36]–[38]. The authors consider the case when the distribution of surface ordinates is described by the normal distribution law function $f(z)$. Due to the stationarity of the random field, it was proposed to calculate the arithmetic mean height according to the following formula:

$$E\{Sa\} \sim Sq\sqrt{\frac{2}{\pi}}. \tag{1.2}$$

The authors note that Relation (1.2) is strictly true only in the case of the normal distribution law at a small signal/noise ratio.

Surface machining traces also affect the wear process. Thus, **Springis,** studying wear on a steel-bronze friction pair, used the parameter RSm_2 in the direction parallel to the machining traces, which is in the friction direction [17]. Figure 1.1 shows the profilogram of the surface of the wear-activating ball after the running-in stage.

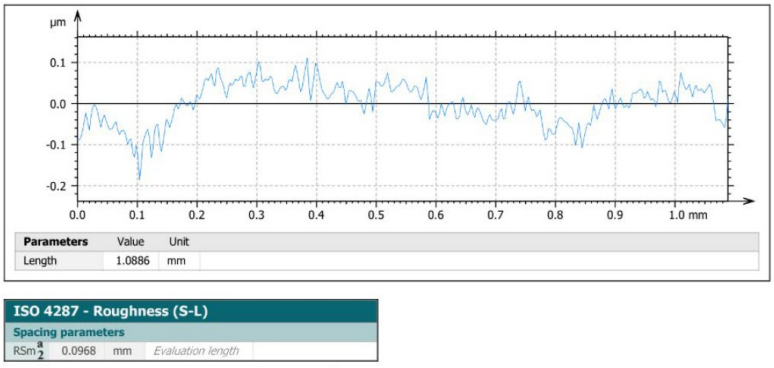

Fig. 1.1. Surface profile of wear-activating ball in the direction of machining traces [17].

The RSm_2 value for the roughness profile is only 0.0968 mm according to the data of the surface computer processing program. This does not correspond at all to the geometry of the profile, for which one wide step with a length of about 0.6 mm can be visually distinguished, determining the RSm_2 in both directions of the profilogram.

Inaccuracy in the determination of the parameter RSm_2 was also noticed in the work of **Buj-Corral**, in which the effect of printing orientation on surface roughness using the fused deposition modeling method (FDM) was investigated [39]. Thus, with an increase in the printing angle from 55 degrees to 85 degrees, the so-called "subroughness" appeared in the roughness profile, which negatively affected the result of RSm_2 reading.

Kumermanis, when studying ground surfaces, also obtained the incorrect values of roughness step. The profile evaluation length of 0.8 mm had only a few intersections with the mean line, which served as "zero" elements; respectively, there were no intersections with the mean line for roughness step determination [40]. In this situation, the problem may be explained by the insufficient evaluation length of the profile.

The peculiarities of the surface texture in different directions also play a great role in friction processes. **Rudzitis** used the anisotropy coefficient *C* in wear calculations, which determines the relationship between the steps of the surface profile perpendicular to and parallel to the machining traces [36], [37]. The author proposed to determine the surface anisotropy according to the following expression:

$$C = \frac{RSm_1}{RSm_2}. \tag{1.3}$$

Accordingly, if the surface is isotropic, $RSm_1 = RSm_2$ and $C = 1$. But if the surface is anisotropic, $RSm_2 \to \infty$, $C \to 0$. This parameter is not standardized but is actively used in surface roughness studies.

Springis, Boiko, et al. proposed to use the standardized 3D roughness parameter *Str* to determine surface anisotropy [41]. In the standard EN ISO 25178-2, the parameter *Str* – surface texture aspect ratio – is defined as the ratio between the horizontal distances of the correlation function fACF(*tx*,*ty*), which are characterized by the fastest and slowest decay of the function in the interval from 0 to 1. A similar approach was used by the 20th century researcher **Husu**, studying the effect of surface roughness anisotropy on wear resistance [38]. The possibility of application of the parameter *Str* in wear calculations needs to be verified, since studies on the identity of the surface texture aspect ratio and the parameter *C* have not been conducted. If the values of the given parameters have a high congruence, then it will be possible to use the parameter *Str* in roughness step calculations.

The volume of worn material is included in several wear calculation models. For the mathematical determination of the given parameter, some authors use a set of 3D and 2D roughness parameters. Thus, **Springis** expressed the total deformed volume as the product of the volume separated from the *i*-th peak by the number of deformed peaks [17]. **Rudzitis** had a different formulation for the volume of worn material [37]. He introduced the parameter *Vu* – the volume of peaks at the surface cross-level *u*. The calculation of the given parameter was also based on the normal random field theory. The author proposed determining the parameter *Vu* by integrating the surface cross-sectional area $A(u)$ by levels, counting from the mean plane. After performing the relevant transformations, it was proposed to calculate the given parameter analytically using the following formula:

$$E\{Vu\} \sim Sq \times Aa \times \left\{ \frac{1}{\sqrt{2\pi}} exp\left(-\frac{c^2}{2Sq^2} \right) - \frac{c}{Sq}\left[1 - \Phi\left(\frac{c}{Sq} \right) \right] \right\}. \tag{1.4}$$

Kumermanis had compared the *Vu* values expressed by Formula (1.4) with experimental data – the parameter *Vm* [40]. The author noted that in the running-in stage ($u < 30$ %) and the normal wear stage ($u \sim 30...70$ %), the *Vu* values are less than *Vm;* only in the catastrophic wear stage, when $u > 70$ %, the values of the *Vm* parameters were close to the theoretical ones. Kumermanis, when comparing the analytically determined values of the material volume with experimental data, did not take into account the difference in units of measurement. Thus, when determining the material volume theoretically according to Formula (1.4), the unit of measurement of the *Vu* parameter is mm^3, while the computer processing program determines the parameter values mm^3/mm^2. Therefore, in order to make conclusions about the possibility of applying Formula (1.4) to determine the material volume, additional research is required.

Due to the fact that wear calculations and analytical formulas for the determination of roughness parameters for surfaces with an irregular character are based on random field theory and the normal distribution law, it is important to determine whether the deviations from the normal distribution law will affect the accuracy of the calculation results.

1.3. Evaluation of the surface roughness ordinates distribution

As mentioned in the previous chapter, several wear calculation models were based on the specific assumption that the roughness of surfaces with an irregular character is described by the normal random function. Such an assumption was made based on studies conducted in the middle of the 20th century on the correspondence of the surface roughness ordinates distribution to the Gaussian distribution. The distribution of the ordinates was checked on probability paper, by correlation functions, the agreement criterion $n\omega^2$ [15], [38], [42], [43], the Pearson and Kolmogorov criteria, asymmetry, kurtosis, and material ratio curve [17]. In addition, the results of the studies indicated a partial correspondence of the ordinate distribution to the normal distribution law.

There are very few modern studies on the correspondence of the surface roughness model to the normal distribution law. **Karkalos** attempted to analyze the surface roughness model after hydroabrasive cutting by comparing the asymmetry *Rsk* and kurtosis *Rku* values with the parameters of the normal distribution function [44]. The difference between the measured and standardized *Rsk* values was more than 100 %, the *Rku* values differed by 40 %, and only a few samples showed a visible coincidence. **Wechsuwanmanee** compared the statistical distribution of the roughness ordinates with the fitted normal distribution curve, analyzing the effect of surface roughness on cold formability in bending processes [45]. The results indicated a close correspondence to the Gaussian distribution. **Quezada**, studying the surfaces of prosthetic dental acrylic resins after manual and mechanical polishing, used the ordinate distribution function and its characteristics *Rsk* and *Rku* to verify the surface model [46]. The author noted that after mechanized polishing, the *Rku* values were close to 3, deviation was about 10 %, but there was a visible asymmetry in the ordinate distribution – the *Rsk* values tended to 1. Based on the authors' studies, it can be concluded that the distribution of the ordinates is only close to normal but does not completely correspond to it. This can be explained by the evaluation of the individual roughness profiles, which cannot fully reflect the character of the 3D surface.

There are many methods for checking the distribution of a random variable for compliance with the normal distribution law. Thus, in **2021, Hernandez** conducted an extensive analysis of existing normality tests, including 55 different methods, and their comparison according to the Monte Carlo power criterion (1–β) to determine the ability of the test to correctly identify the sample [47]. Hernandez summarized 20 studies from 1990 to 2021, in which the power of normality tests was compared. He considered the results obtained only for a small sample ($n < 35$), because the differences in power between the tests were the most obvious. The best results were shown by the Shapiro-Wilk regression test, the Anderson-Darling test based on the empirical cumulative distribution function, and the Hosking L-moment test.

When measuring the surface roughness geometry, a surface consisting of millions of points is generated, so the power of most normality tests will reach 100 %. And since in any case the ordinates distribution function of surfaces with an irregular character will have a single peak and will decrease indefinitely with argument increase in absolute value, the density of the distribution will differ from the normal one mainly in the values of skewness and kurtosis. Therefore, if there is a known assumption about the type of deviation from the normal distribution law, i.e. when considering a distribution whose skewness and kurtosis values differ from those typical of a normal distribution, it is useful to use moment-based tests. This means that the evaluation of the surface roughness ordinates distribution can be limited by the determination of the skewness *Ssk* and kurtosis *Sku* values.

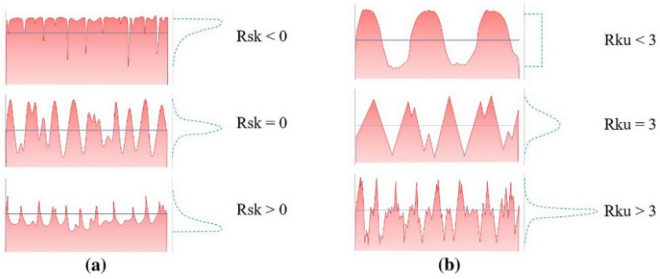

Fig. 1.2. Representation of the surface ordinates distribution depending on the values of skewness (*Rsk*) and kurtosis (*Rku*) [48].

1.4. Influence of surface computer processing operations on the precision of determining the roughness parameters

After performing a measurement experiment of surface roughness, it is very important to process correctly the topography taken in order to obtain an accurate 3D and 2D surface roughness geometry and a series of parameters that reveal the surface features and characterize its exploitative properties [49], [50]. For these purposes, it is necessary to level the surface and/or remove form to generate a mean plane/mean line for determining the roughness parameters [51]. These operations have a primary impact on the surface roughness geometry. Computer processing programs such as MCube Map Ultimate, TalyMap, MountainsSPIP, etc. offer several types of leveling: by the least squares method – LSP or TLSP leveling; by the minimum zone method – MZP leveling; as well as by leveling each line individually to align them on the same flat reference – line by line leveling. The surface roughness standards ISO 25178 and 21920 give recommendations and explanations for surface filtering and its sequence, but do not define which operators and filters should be applied for a specific surface type.

Nečas has conducted extensive research on how leveling changes the result of 2D roughness measurements, and how to avoid it [52], [53]. Nečas illustrated profile leveling with 1st, 2nd and 3rd order polynomials, where background adjustment removed not only the true

background B, but also the roughness components (Fig. 1.3). Therefore, the roughness parameters of the leveled surface have reduced values.

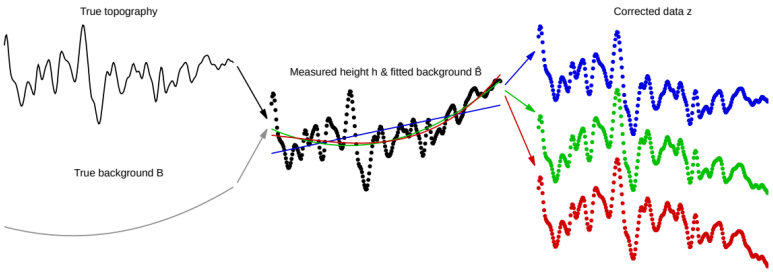

Fig. 1.3. General scheme of how the adjusted background distorts the surface geometry data [53].

Because the wear calculations include 2D roughness step parameters, their values have to be determined by performing separate 2D measurement experiments or by extracting individual profiles from the 3D leveled surface. But sometimes, individual 2D measurements are physically impossible due to the peculiarities of the surface texture and other factors [54]. In turn, the ISO 25178-3 standard warns [55] that profile and texture filtering with the same filter type and cut-off/nesting index can give completely different results. Studies on the influence of 3D surface leveling on the geometry of individual profiles were not found when analyzing the relevant literature. Therefore, it is important to determine a suitable leveling operation that would preserve the geometry of the profiles. Among them, there is a topical issue of the mutual arrangement of the profile mean line and surface mean plane, because from the unified surface description, the reference bases of the 2D roughness parameters – the mean lines, must be at the level of the surface mean plane, only then the 2D parameters will characterize the 3D surface, but it, in turn, is also affected by the leveling operations.

1.5. Conclusions

According to the literature analysis, the following problems can be identified related to the application of surface roughness parameters.

1. **Wear calculations of friction surfaces.**
   1.1. Several wear calculation models with integrated roughness parameters are limited by:
   - 2D roughness parameters;
   - assumption of the compliance of the ordinate distribution with the normal distribution law;
   - one specific type of contact.

   1.2. When performing wear simulation and calculation in the finite element environment, in several cases, Archard and Fleischer wear calculation models are used, and the type of friction pair contact – smooth surface-smooth surface is chosen, which reduces the reliability of the results.

2. **Determination of roughness parameters.**
   2.1. The influence of the ordinate distribution on the calculation of the arithmetic mean height *Sa* is not specified.
   2.2. The computer processing program gives reduced values of the roughness step RSm_2.
   2.3. The correspondence of the surface texture aspect ratio *Str* to the anisotropy coefficient *C* has not been checked.
   2.4. Correct analytical determination of the material volume *Vm* has not been performed.
3. **Computer processing of 2D and 3D surface geometry.**
   3.1. The influence of 3D surface leveling on the geometry of individual profiles has not been studied.
   3.2. The question of the mutual location of the profile mean line and surface mean plane, which influences the determination of 2D roughness parameters, has not been studied.
4. **Evaluation of the roughness ordinates distribution law.**
   4.1. The results of the normality tests indicate a partial compliance of the ordinates distribution to the normal distribution law, which may limit the application of equations based on random field theory for the determination of the roughness parameters.

Hypothesis: Specified determination and integration of the 3D and 2D surface roughness parameters, as well as the use of individual material fatigue characteristics in wear intensity calculations and prediction, will increase the reliability of the results for elastic and plastic contact cases.

2. EXPERIMENTAL DETERMINATION OF SURFACE ROUGHNESS

2.1. 3D and 2D roughness measurement experiment

In this Thesis, the process of measuring the 3D and 2D surface roughness parameters was carried out using the contact method. The Mitutoyo Formtracer avant S-3000 profilometer was selected for the experiments. The given device is equipped with a standard stylus 12AAC731 with a diamond tip; the tip radius is 2 µm, the cone angle is 60 degrees, and the measuring force is 0.75 mN.

The TESA RUGOTEST Roughness Comparison Specimens from stainless nickel and other experimental samples from steel were selected for the experiments. Since surfaces with irregular roughness were studied in this Thesis, specimens after abrasive treatment and electric erosion were selected for measuring experiments. For each specimen, surfaces with different arithmetic mean heights and cut-off values were studied.

For 3D roughness measuring experiments, the dimensions of the evaluation area (square edges) were defined: $L = 5l$ (according to the recommendations of the ISO 25178-2 and ISO 21920-2 standards); for 2D measurements, the evaluation length of roughness profile was limited by the sample dimensions, i.e. the maximum possible evaluation length in the X and Y-axis directions was selected.

2.2. Correct selection of texture leveling operation

The data obtained from surface topography after the 3D roughness measurement experiments were processed in the McubeMapUltimate 10 computer program [56]. Different leveling operations were applied to the studied surfaces with the aim of finding the optimal variant for preserving the surface geometry and, accordingly, ensuring the accuracy of the roughness parameters.

Analysis of the 3D geometry of the ground surface and the extracted profiles perpendicular and parallel to the machining traces before computer processing indicates that the profiles in the X-axis direction do not have a pronounced skew, whereas in the second direction, there is a clearly pronounced slope, which does not allow an adequate assessment of the roughness step in this direction. With the help of the function “Subtract”, the reference lines (least squares lines) of the original profiles were obtained in directions perpendicular and parallel to the machining traces (Fig. 2.1).

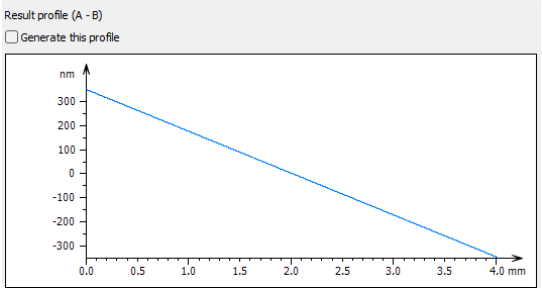

a

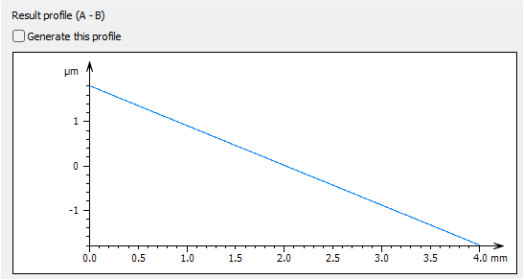

b

Fig. 2.1. Slope of the reference line of the original profile:
a – perpendicular to the machining traces; b – parallel to the machining traces.

Comparing the profiles before and after leveling it can be concluded that the slope of the reference line of the original X-axis profile is several times smaller in comparison with the Y-axis profile, and the ordinates distribution of the profile in relation to its mean line is minimally changed after leveling. Accordingly, for the Y-axis profile before leveling the number of intersections with the mean line will give an erroneous value of the roughness step RSm_2. To solve the given problem and choose the optimal type of profile leveling, different types of leveling operations were performed for a freely selected profile of the Rugotest 104 surface N.6 – LSL, TLSL and MZL leveling. Comparing the profile roughness parameters before and after leveling (Table 2.1), it can be seen that the values of the arithmetic mean height *Ra* after leveling decrease, whereas the values of the roughness step *RSm* increase and in this case correspond to the profile geometry, which is provided by the least square leveling method.

Table 2.1

Roughness Parameters of the Original Profile *P* and LPveled profiles

Parameter	*P*	P_{LSLl}	P_{TLSLl}	P_{MZLl}
Ra	1.06	0.57	0.57	0.66
RSm	1.45	1.71	1.71	0.81

The next step was surface leveling, using different leveling operations, with further profile extraction. To check the degree of coincidence of the originally leveled profile with the extracted one from the differently leveled surface, the parameter *RMS* (using the function "Subtract") – root mean square deviation, which was calculated over the length of the overlap zone, was used. Table 2.2 shows the *RMS* values for surface profiles depending on leveling type. The smaller the *RMS* value, the higher the degree of coincidence of the profiles. Within the study, 100 profiles of the ground surface in the X-axis direction and the same number of profiles in the Y-axis direction were selected for comparison in order to check which of the directions is more affected by 3D leveling operations.

Table 2.2

RMS Values for Profiles Depending on the Leveling Type

#	Type of leveling	RMS_{vid}, nm (X-axis)	RMS_{vid}, nm (Y-axis)
1	LSPL	1.45e-7	2.59e-7
2	TLSPL	1.28e-7	2.66e-7

Table 2.2 (continued)

#	Type of leveling	RMS_{vid}, nm (X-axis)	RMS_{vid}, nm (Y-axis)
3	MZPL	1.87e-7	2.78e-7
4	Leveling line by line – subtract the mean + LS-polynomial, $P = 1$	**2.35e-10**	3.54e-7
5	Leveling column by column – subtract the mean + LS-polynomial, $P = 1$	1.09e-6	**2.89e-10**

According to the data in Table 2.2, it can be concluded that leveling line by line + LS-polynomial $P = 1$ gives the most accurate match with the X-axis originally leveled profiles, while leveling column by column + LS-polynomial $P = 1$ gives the most accurate match with the Y-axis originally leveled profiles. Due to the fact that the 3D geometry of the surface must be taken perpendicular to the processing traces, choosing leveling column by column is not correct, because artificially generated extreme peaks will appear on the surface. Accordingly, based on the RSM_{vid} value, leveling line by line together with LS-polynomial is the best variant.

2.3. Determination of the mutual location of the profile mean line and surface mean plane

In this section, it is graphically substantiated how the mean lines of the profiles are related to the mean plane of the surface and how their location is affected by leveling operations. For this purpose, in the MCubeMAP Ultimate 10 computer program, two grooves were artificially created for the 3D surface after various types of leveling in order to compare the location of the profiles' mean lines in the X-axis and Y-axis directions in relation to the mean plane of the surface (Fig. 2.2).

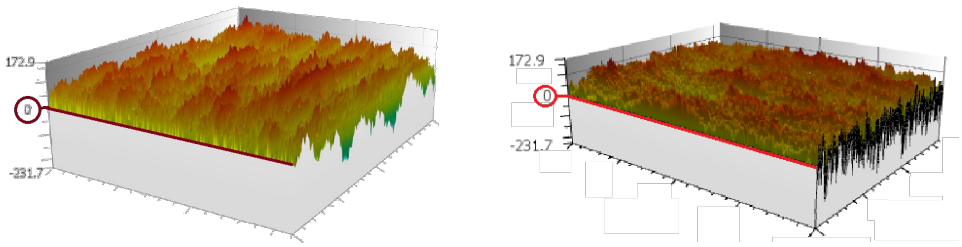

a b

Fig. 2.2. Surfaces with artificially created grooves after LSPL:
a – perpendicular to the machining traces; b – parallel to the machining traces.

For the given surfaces, all profiles in mutually perpendicular directions were obtained with the help of the computer program function "Extract series of profiles". Analysis of the profiles indicates that the location of the groove for all profiles in the Y-axis direction varies from –0.06 µm to 0.06 µm in relation to their mean lines. In turn, the amplitude of fluctuations of groove location for the X-axis profiles is significantly smaller, from –0.015 µm to 0.025 µm in relation to their mean lines.

To select the optimal leveling method, the mutual locations of the surface mean plane and the profile mean lines after different leveling operations were compared, determining the maximum deviations of the profile mean lines from the mean plane h_{x_max} and $h_{y\_max,}$ in relation to the surface maximum height, *Sz*.

Table 2.3 shows the maximum deviations of the profile mean lines from the mean plane in the directions parallel and perpendicular to the processing traces for differently machined surfaces. Thus, when performing leveling by the *least squares method*, deviations of the mean lines from the location of the mean plane are visible in both directions: the deviation along the X-axis reaches 6 %, but along the Y-axis – 17 %. *Line-by-line leveling* ensures complete coincidence between the mean lines of the X-axis profiles and the mean plane, but *column-by-column leveling* – complete coincidence between the mean lines of the Y-axis profiles and the mean plane. When performing *line-by-line + PL leveling*, the h_{i_max}/Sz value for isotropic surfaces in the longitudinal direction is significantly smaller than for anisotropic ones. The analysis results indicate that the trend of the leveling effect remains for all samples. Taking into account the direction of measurement and the complete coincidence between the mean plane and the mean lines of the X-axis profiles, *leveling line by line together with the LS-polynomial* is the optimal variant for preserving the surface geometry.

Table 2.3

Maximum Deviation of the Profiles' Mean Lines from the Surface Mean Plane Depending on the Type of Leveling

Type of treatment	Axis	Maximum deviation h_{i_max}/Sz, depending on the leveling type, %				
		LSPL	Line by line	Line by line +PL	Column by column	Column by column +PL
Surface grinding	x	4.9	0	0	10.5	6.2
	y	16.1	17.8	17.0	0	0
Cylindrical grinding	x	5.6	0	0	11.2	7.1
	y	15.2	18.2	17.7	0	0
Electro erosion	x	1.8	0	0	13.2	9.6
	y	10.6	3.8	3.5	0	0
Shot blasting	x	2.2	0	0	12.1	9.3
	y	11.4	4.5	4.1	0	0
Grit blasting	x	3.2	0	0	12.8	10.1
	y	12.1	6.2	5.8	0	0
Polishing	x	6.3	0	0	11.8	7.3
	y	17.4	18.7	18.2	0	0
Lapping	x	4.3	0	0	11.1	7.1
	y	15.8	17.3	16.5	0	0

2.4. Conclusions

1. The type of leveling has a different effect on the mutual location of the surface mean plane and the profile mean lines.

1.1. The complete coincidence between the X-axis profiles' mean lines and the surface mean plane is observed when choosing the *line-by-line leveling.*

1.2. The complete coincidence between the Y-axis profiles' mean lines and the surface mean plane is observed when choosing the *column-by-column leveling.*

1.3. In the case of *LSP leveling*, the deviation between the mutual location of the surface mean plane and the profiles' mean lines is observed in both the X and Y-axis directions.

2. Taking into account the parameter *RMS* value and the analysis of the mean plane and the mean line mutual location, it was concluded that the leveling function *leveling line by line together with LS-polynomial* is the most optimal variant for preserving the surface geometry.

3. CALCULATIONS OF 3D AND 2D SURFACE ROUGHNESS PARAMETERS

3.1. Checking the compliance of the irregular surface roughness model with the normal distribution law

In this section, the surface roughness model of the samples was checked by comparing the theoretical values of the model parameters with experimental data. Figure 3.1 shows the histograms of the roughness ordinates distribution for surfaces with an irregular character after abrasive treatment. After visual analysis of the histograms, in the first approximation, it can be assumed that the ordinates distribution corresponds to normal, which is indicated by the bell shape of the histogram with an unexpressed asymmetry.

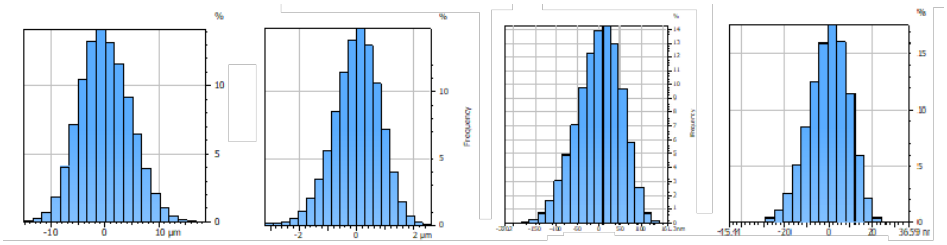

a b c d

Fig. 3.1. The ordinates distribution histograms of surfaces with an irregular character: a – grit blasting; b – shot blasting; c – surface grinding; d – polishing.

The conformity of the surface ordinates distribution function with the normal distribution law was checked according to two criteria: *Ssk* – asymmetry, and *Sku* – kurtosis.

Figure 3.2 shows the experimentally obtained asymmetry values of the roughness ordinates distribution function and the theoretical *Ssk* (line at the zero value). When comparing the experimentally obtained values of the parameter *Ssk* with the theoretical one, it can be concluded that for no sample does the *Ssk* value fall within the relative deviation +/– 10 %, it reaches 100 %. The measured values of the parameter *Ssk* are in the interval $-0.58 < Ssk_{exp} < 0.18$.

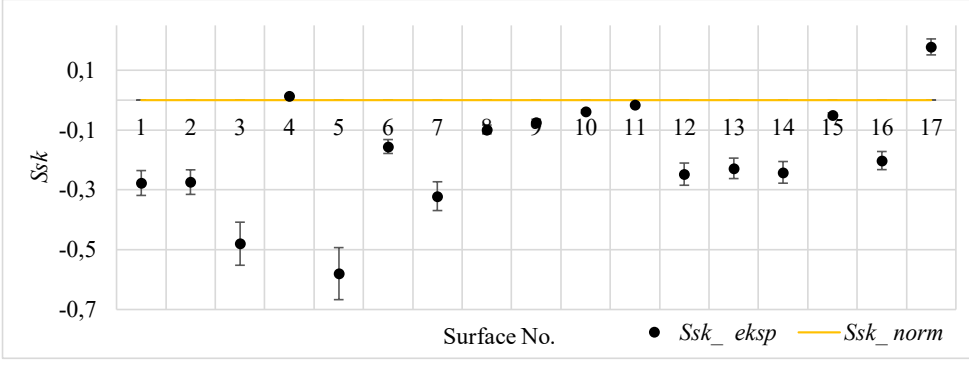

Fig. 3.2. Experimental and theoretical values of the parameter *Ssk*.

Figure 3.3 shows the values of the roughness parameter *Sku*. As mentioned above, according to the normal distribution law, the kurtosis value should be equal to 3. Graphical analysis shows that for all surfaces, the difference in *Sku* theoretical and experimental values reaches +/– 13 %. The measured values of the parameter *Sku* are in the range $2.7 < Sku_{exp} < 3.4$.

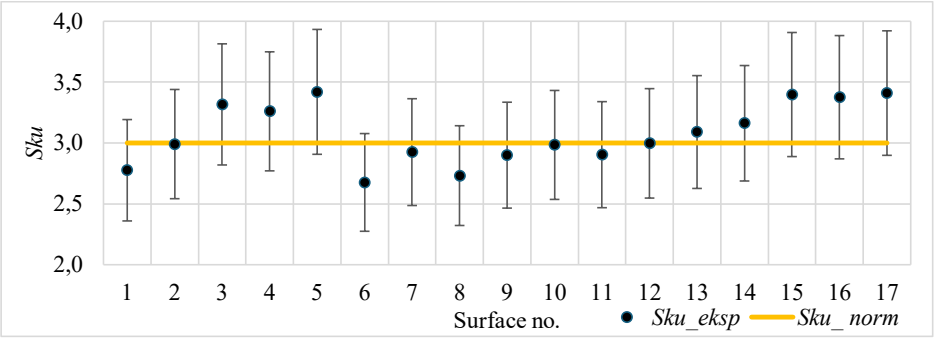

Fig. 3.3. Experimental and theoretical values of the parameter *Sku*.

When comparing the 3D and 2D roughness parameters, it can be concluded that the *Rsk* values perpendicular to the processing traces quite accurately coincide with the *Ssk* values and the difference is less than 15 %, while in the longitudinal direction the *Rsk* values correspond to the *Ssk* values only for those samples which do not have a pronounced direction of the machining traces, i.e. surfaces after electro erosion, grit blasting, shot blasting. The kurtosis values of the surface ordinates distribution function are very close to the *Rku* values perpendicular and parallel to the processing traces, but the exception is also surfaces with a high degree of anisotropy, for which the *Rku* values in the Y-axis direction differ from the *Sku* values by more than 15 %. This disparity can be seen in Fig. 3.4 a.

When performing separate 2D roughness measurements at an increased evaluation length – $L = 80l$, a completely different distribution of roughness ordinates can be observed. In Fig. 3.4 b, the bell-shaped distribution of the roughness ordinates is clearly visible. In this case, $Rsk_2 = -0.25$, $Rku_2 = 3.25$. Such differences in parameter values can be explained by the limited evaluation length for the Y-axis profiles.

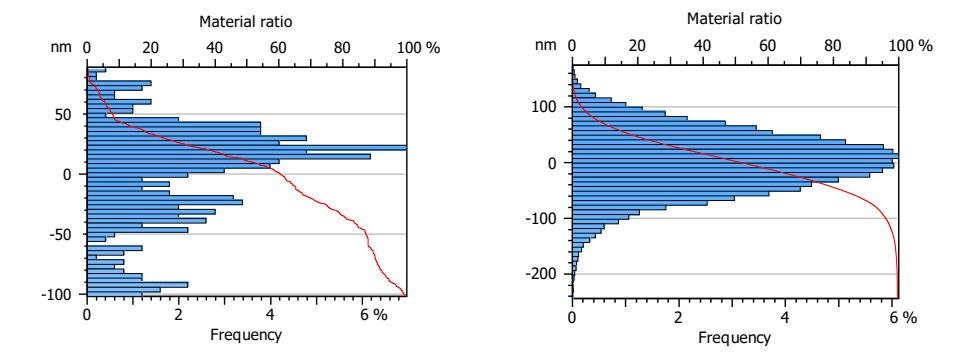

a b

Fig. 3.4. Distribution of points of the ground surface profile in the direction parallel to the machining traces: a – $L = 5l$; b – $L = 80l$.

3.2. Surface arithmetic mean height *Sa*

Surface arithmetic mean height, *Sa,* characterizes the height properties of the microrelief. As mentioned in Section 1.2, in the case of the normal distribution of ordinates, this parameter is determined by Formula (1.2). Because in practice, the roughness ordinates of surfaces with an irregular character are not ideally distributed by normal distribution law, it is important to understand how the asymmetry *Ssk* and kurtosis *Sku* of the surface ordinates distribution function affect the values of the arithmetic mean height *Sa.*

The random process $z(x,y)$ can be viewed as the normed random process $z'(x,y)$. The density of the ordinates distribution with $E = 0$ and $D = 1$ can be approximated by the Edgeworth series [15]:

$$f_2(z') = f(z') - \frac{Ssk}{3!}\Phi^{(4)}(z') + \frac{(Sku-3)}{4!}\Phi^{(5)}(z') - \cdots, \quad (3.1)$$

where $f(z')$ is the normal distribution density of the random variable z', and $\Phi^{(i)}(z')$ is the i-th derivative of the Laplace function.

Based on the relationship between the derivatives of the Laplace function and the Hermite polynomials $Hn(p)$ [15], the fourth and fifth derivatives of the Laplace function were determined. After transformations, the following formula for calculation of the arithmetic mean height was obtained:

$$E_2\{Sa\} = E\{Sa\} \times \left(1 - \frac{(Sku-3)}{4!}\right). \quad (3.2)$$

If the distribution of the surface ordinates is normal, then Relationship (3.2) passes into Relationship (1.2). Analysis of the obtained relationship indicates that the value of $E_2\{Sa\}$ depends on the kurtosis. The values of the asymmetry *Ssk* appear in the process dispersion, and at a constant dispersion, *Ssk* do not affect $E_2\{Sa\}$.

$$E_2\{Sa\} = Sq\sqrt{\frac{2}{\pi}} \times \left(1 - \frac{(Sku-3)}{4!}\right). \quad (3.3.)$$

In Fig. 3.5, it is seen that the effect of the kurtosis value is not so significant, since *Sku* values greater than 1.2 change the value of the roughness parameter *Sa* only by 5 %. However, the results of roughness measurement experiments indicate that the *Sku* values are in the range of 2.7...3.4; therefore, theoretically, without loss of accuracy, the normal distribution law function can be used as a basis.

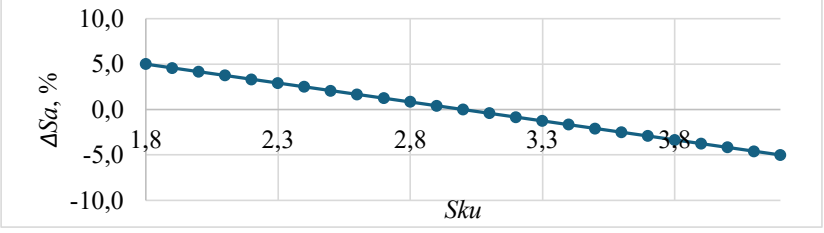

Fig. 3.5. The influence of the kurtosis of the ordinates distribution function on the value of the roughness parameter *Sa.*

The next stage is to compare the experimentally determined values of the arithmetic mean height with those calculated according to Equations (1.2) and (3.3).

Table 3.1

Comparison of Experimentally and Analytically Determined Values of the Parameter *Sa*

Type of treatment	No.	Sa_{eksp}, µm	Sa_{teor}, µm	Sa_{Rudz}, µm	$\lvert\Delta Sa_{teor}\rvert$, %,	$\lvert\Delta Sa_{Rudz}\rvert$, %,
Surface grinding	1	0.042	0.048	0.048	0.01	0.27
	2	1.419	1.414	1.414	0.33	0.36
	3	3.307	3.291	3.335	0.48	0.84
Cylindrical grinding	4	0.049	0.049	0.049	0.14	0.95
	5	0.111	0.112	0.114	0.98	2.71
	6	1.202	1.198	1.182	0.37	1.72
Electro erosion	7	0..733	0.728	0.726	0.76	1.08
	8	1.199	1.197	1.184	0.14	1.26
	9	2.905	2.904	2.892	0.05	0.47
Shot blasting	10	0485	0.485	0.484	0.14	0.20
	11	1.263	1.265	1.260	0.15	0.25
	12	3.429	3.426	3.425	0.09	0.11
Grit blasting	13	0.501	0.499	0.502	0.36	0.25
	14	1.067	1.064	1.072	0.25	0.43
	15	2.417	2.393	2.442	0.99	1.00
Polishing	16	0.205	0.207	0.210	0.75	2.31
Lapping	17	0.021	0.021	0.022	0.83	2.52

According to the data in Table 3.1, it can be concluded that the calculated values of the arithmetic mean height according to Equation (3.3) exactly coincide with the experimentally determined ones, and the deviation from the theoretical values is less than 1 %. When calculating the roughness parameter *Sa* according to Formula (1.2) at *Sku* = 3, the deviation reaches 3 %.

Equation (3.3) differs from the corresponding expression for the determination of the 2D parameter *Ra* only by the root mean square deviation. If its values are the same for both the field and the process, then it can be concluded that the profile mean line coincides with the level of the surface mean plane. In Chapter 2, it was justified that there is a certain offset between the surface mean plane and the profiles' mean lines. To check how this offset affects the values of the parameter *Ra*, for all sample series after leveling line by line + LS polynomial 1, the arithmetic mean height *Sa* and 2D parameters Ra_1 and Ra_2 in directions perpendicular and parallel to the machining traces were determined, where the values of Ra_1 and Ra_2 are the average values of all X-axis profiles and Y-axis profiles.

The results of the study indicate that the values of the profile parameter *Ra* in the direction perpendicular to the machining traces quite accurately coincide with the values of the parameter *Sa*, the maximum deviation reaches only the 5 % limit. This is a particularly good indicator, which can be used to conclude that the profile mean lines coincide with the surface mean plane level. In turn, for surfaces with pronounced anisotropy, the parameter *Ra* values in the direction parallel to the processing traces differ from the 3D arithmetic mean height, and the deviation from the *Sa* values reaches 34 %. This can be explained by the offset of the Y-axis mean lines relative to the surface mean plane.

3.3. Surface texture aspect ratio *Str*

In this Thesis it was proved that for the evaluation of anisotropy, it is useful to use the standard EN ISO 25178-2 parameter *Str* – surface texture aspect ratio, which is defined as the ratio between the horizontal distances of the correlation function $f_{ACF(tx,ty)}$, which are characterized by the fastest and slowest decay of the function in the interval from 0 to 1. This definition can be written as follows:

$$Str = \frac{t_x, t_y^{\min} \in R\sqrt{t_x^2 + t_y^2}}{t_x, t_y^{\max} \in R\sqrt{t_x^2 + t_y^2}}, \tag{3.4}$$

$$Str = \frac{R\min}{R\max}, \tag{3.5}$$

where $R = \{(t_x, t_y): f_{ACF}(t_x, t_y) \leq s\}$, and $R_{\min}$ and $R_{\max}$ are the main radii of the central threshold portion of the correlation function.

The surface correlation function in the case of general anisotropic surface roughness can be oriented differently relative to the coordinate axes X and Y (Fig. 3.6).

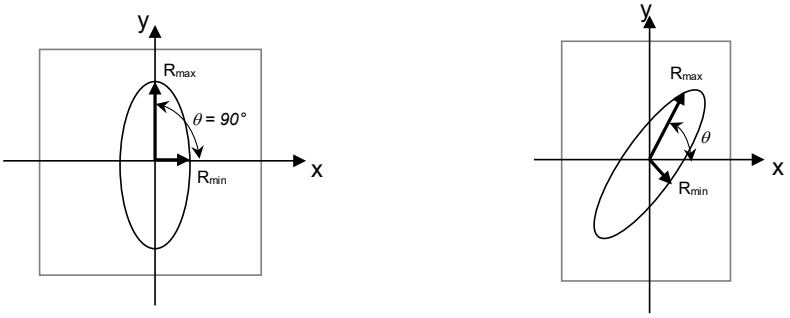

a b

Fig. 3.6. Schematic arrangement of the main radii of correlation functions:
a – the correlation function is oriented along the X and Y axes; b – the correlation function is not oriented along the X and Y axes.

The magnitude of the decrease in the value of the correlation function is characterized by the correlation length, *Sal* or $R_{\min}$. So, if we assume that the correlation function $f_{\mathrm{ACF}}(t_x,t_y)$ is oriented along the main directions of an anisotropic rough surface, then $R_{\min} = \tau_{kx}$ in the X-axis direction and $R_{\max} = \tau_{ky}$ in the Y-axis direction, since in the direction perpendicular to the machining (friction) traces the surface profile has a higher density of irregularities, at which the correlation function also decays faster. According to Equation (3.5):

$$Str = \frac{\tau_{kx}}{\tau_{ky}}. \tag{3.6}$$

It is important to note that in the standard EN ISO 25178-2, the autocorrelation function is intended to be determined at the level $0 \leq s \leq 1$ (recommended $s = 0.2$). However, at any level *s,* the ratio retains its principal value; therefore, without losing the general approach, Formula (3.6) can be used to characterize the parameter *Str* at any value of *s*. Then, using studies

of the correlation function of an irregular rough surface profile [36], [37], for a monotonically decreasing correlation function:

$$\tau_k = \frac{\tau_{kn}}{E\{n(0)\}}, \tag{3.7}$$

where τ_{kn} is the normed value of the correlation interval (it is a constant for a specific correlation function [36]); and $E\{n(0)\}$ is the number of zeros per unit length.

According to Formula (3.6) for a decreasing correlation function:

$$Str = \frac{E\{n_2(0)\}}{E\{n_1(0)\}}, \tag{3.8}$$

where indices 1 and 2 characterize the transverse and longitudinal profiles, respectively.

The following relationship exists between the number of zeros per unit length and mean roughness profile element spacing:

$$E\{n(0)\} = \frac{2}{RSm}. \tag{3.9}$$

Accordingly, Equation (3.8) can be rewritten as follows:

$$Str = \frac{RSm_1}{RSm_2}. \tag{3.10}$$

Comparing the obtained equation with Equation (1.3), we obtain a theoretical justification for the application of the surface texture aspect ratio in the assessment of surface anisotropy:

$$Str = C. \tag{3.11}$$

Since Equation (3.11) is suitable for cases when the surface mean plane coincides with the profiles' mean lines, it is important to accurately determine the RSm_2 value for surfaces with an irregular character, because profiles' mean lines in the direction parallel to the processing traces will have deviations from the mean plane location after leveling.

3.4. Mean roughness profile element spacing *RSm*

In the ISO 21920-2 standard, it is defined that the parameter *RSm* is calculated at a certain vertical limit (height discrimination *H*) – at 10 % of *Rp* (mean profile peak height) and 10 % of *Rv* (mean profile pit depth) at the standardized evaluation length. In turn, as mentioned above, for surfaces with an irregular character, not all profiles are suitable for evaluation of the roughness step in the longitudinal direction, since the number of profile intersections with the mean line may be insufficient to identify profile elements. However, there are many cases when the number of profile intersections with the mean line is too large due to local subroughness. In this case, the values of the average roughness step RSm_2 will be greatly reduced. Within the Doctoral Thesis, it was determined that to solve the given problem, it is necessary to choose the appropriate height discrimination that would exclude unnecessary components from the roughness step, because by increasing the height discrimination to 30–40 %, the RSm_2 values of the profiles begin to correspond to the real value. Since each profile will have a different height discrimination in this Thesis, it was proposed to determine the RSm_2 value using the waviness step, because its size at a correctly selected cut-off is comparable to the roughness

profile step. It is important to note that in this case, the waviness profile reflects not the shape deviation that occurs during the mechanical processing of the part, but directly the roughness step size in the direction of the machining traces. With the help of the function "Filtered profiles", it is possible to obtain a waviness profile by selecting a r*obust Gaussian filter*, which is not affected by local surface defects, measurement noise, extreme pits and peaks.

To check the correspondence of the WSm_2 parameter value to the roughness step RSm_2, 100 profiles were selected, for which RSm_2 values at the thresholds H = 30–80 % and WSm_2 values at H = 10 % were determined, using computer program calculations. The results of the study showed that the WSm_2 parameter values coincide very well with RSm_2 at H = 30–40 %, the difference in the results is less than 5 %. In turn, there is a question: what cut-off value should be chosen for the waviness profile not to lose important elements and vice versa – not to repeat the sub-roughness. Figure 3.7 shows waviness profiles with different cut-offs. The larger the L-filter value, the wider the waviness step will be.

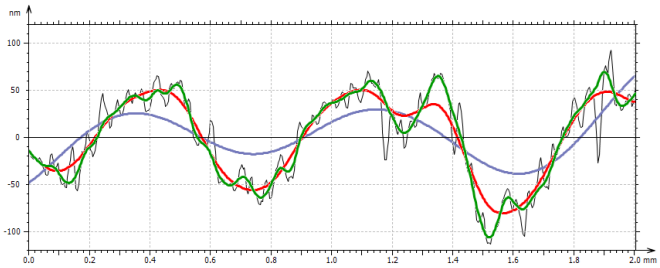

Fig. 3.7. The effect of the cut-off size on the waviness step.
λc = 0.08 mm (green), λc = 0.25 mm (red), λc = 0.8 mm (blue).

After comparing the values of the parameters RSm_2 and WSm_2 at different cut-offs, it was concluded that for waviness profiles, a cut-off of one unit smaller than the standardized one should be chosen.

The next point was the comparison of WSm_2 values for profiles after 2D and 3D measurements. Based on experimental data, it can be concluded that for profiles with an increased evaluation length, the values of the parameter WSm_2 are greater than after 3D measurements, the difference is 8–25 % (on average 16 %), which can be explained by the deviation of the profiles' mean lines from the mean plane location. The question arises, which of the WSm_2 values should be chosen for wear intensity calculations? Here, it is important to note the role of the roughness parameter *Str*. In this Thesis, the comparison between the ratio Str_v of all extracted X and Y-axis profiles of the filtered surface with the surface texture aspect ratio *Str*, and the ratio Str_p of the steps RSm_{1_p} and WSm_{2_p} of the separately taken profiles with the same parameter *Str* was made. For this purpose, 2D roughness measurement experiments of the X-axis profiles were additionally performed at the increased evaluation length. Comparison of the roughness step values perpendicular to the processing traces shows that the RSm_1 values after 3D and 2D measurements coincide very precisely; the difference in values is a maximum of 5 %. Accordingly, it can be concluded that the RSm_{1_v} values of the profiles extracted from the leveled surfaces can be used in surface anisotropy assessment ($RSm_{1\_v} \approx RSm_{1\_p}$).

In Fig. 3.8, three combinations of surface texture aspect ratio are shown. It can be concluded that the values of the parameter WSm_{2_p} ensure complete coincidence between the roughness step ratio and the parameter *Str*.

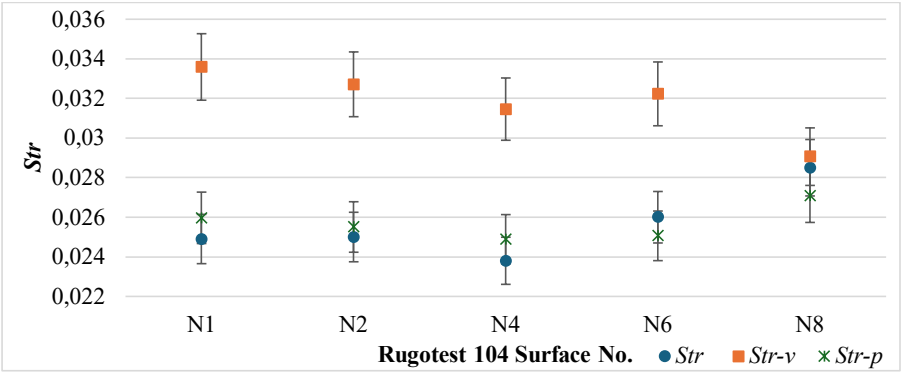

Fig. 3.8. Correspondence of the roughness steps ratio to the surface texture aspect ratio *Str*.

Based on the results obtained in the study, it was proposed to use the correction coefficient $k_{pr} = 1.16$ for determination of the surface roughness step parallel to the machining traces at the evaluation length $L = 5l$, which takes into account the deviations of the profile mean lines from the mean plane. Accordingly, the roughness step RSm_2' can be determined by the following equation:

$$RSm_2' = k_{pr} \times WSm_2. \tag{3.12}$$

3.5. Material volume *Vm*

The volume of the microirregularities of a rough surface at level *c*, counting from the mean plane, is an important parameter in the wear calculations. The volume of the surface material at a given level expresses the volume of the deformed material during the friction process. The roughness parameter *Vm* of the ISO 25178-2 standard is expressed in mm^3 per unit area mm^2, while in the calculations of the wear intensity, it is important to know the absolute volume of the deformed material, expressed in mm^3. For this purpose, it is useful to use the function "Slices" of the MCubeMap Ultimate 10 software, with the help of which the generated surface is divided into two parts: material and voids. By choosing the required level (designated as "Threshold" in the program), it is possible to obtain the required values of absolute material volume, *Vm'* (volume of material), expressed in μm^3.

Based on the research of Rudzītis, the average material volume can be obtained analytically by integrating the surface cross-sectional area $A(c)$ by levels, counting from the mean plane [37]:

$$Vm = \int_c^{\infty} A(c)dc, \tag{3.13}$$

where $A(c)$ is cross-sectional area, mm^2.

By integrating the cross-sectional area, determined by the Laplace transform, there is a possibility to obtain the mathematically expected value of the material volume:

$$E\{Vm\} = Sq \times Aa \times \left\{\frac{1}{\sqrt{2\pi}} exp(-0{,}5\gamma^2) - \gamma[1 - \Phi(\gamma)]\right\}, \quad (3.14)$$

where γ is relative deformation level, $\gamma = c/Sq$

Expression (3.14) indicates that the material volume *Vm* changes depending on the relative deformation level γ. When γ changes from $-\infty$ to $+\infty$, the volume of the material decreases. At γ values $1 < \gamma < 3$, it can be assumed that the volume of deformed material does not change according to a linear law.

Calculations of the material volume and comparison with experimental data were performed for all studied samples (see Table 3.2). The results show that at deformation levels $\gamma = -3 \ldots 0$ the experimental and theoretical values of the material volume coincide very precisely, the relative deviation $|\Delta V_m'| < 4\%$. At $\gamma = 1$ for several samples, the difference is less than < 10 %, while at deformation level $\gamma > 1$, the difference between the calculated and experimentally determined value reaches 100 % in some cases. This could be explained by the insufficient evaluation area of the sample surface; the experimentally determined material volume *Vm'* at $\gamma > 1$ is less than the theoretical one.

Table 3.2

Comparison of Calculated and Theoretical Values of the Roughness Parameter *Vm'* at Different Relative Deformation Levels

Type of treatment	No.	$\lvert\Delta V_m'\rvert$ at $\gamma = -3$, %	$\lvert\Delta V_m'\rvert$ at $\gamma = -2$, %	$\lvert\Delta V_m'\rvert$ at $\gamma = -1$, %	$\lvert\Delta V_m'\rvert$ at $\gamma = 0$, %	$\lvert\Delta V_m'\rvert$ at $\gamma = 1$, %	$\lvert\Delta V_m'\rvert$ at $\gamma = 2$, %	$\lvert\Delta V_m'\rvert$ at $\gamma = 3$, %
Surface grinding	1	0.07	0.18	0.15	–0,15	–2	–36	–78
	2	0.05	0.26	1.04	0.36	–15	–60	–86
	3	0.02	0.57	2.02	–1.82	–25	–65	–96
Cylindrical grinding	4	0	0	1	1	–4	–37	–70
	5	0.18	0.83	1.58	–3.74	–25	–46	–68
	6	0	0	1	2	–8	–50	–100
Electro erosion	7	0.02	0.25	1.25	1.06	–10	–70	–99
	8	–0.01	–0.01	0.42	1.21	–6	–42	–93
	9	0.00	0.04	0.23	0.44	–4	–26	–78
Shot blasting	10	0.01	0.01	0.18	0.07	–3	–8	0
	11	0.01	–0.03	0.14	0.21	–1	–9	–51
	12	0.02	0.20	1.04	0.10	–10	–51	–95
Grit blasting	13	0.03	3.04	0.94	–0.15	5	–59	–66
	14	0.03	0.24	0.84	–0.36	3	–43	–86
	15	0.04	0.30	0.87	–1.52	–9	–14	198
Polishing	16	0	0	1	–2	–7	4	–99
Lapping	17	0	0	–1	–2	5	56	290

3.6. Conclusions

Results regarding the compliance of the irregular surface roughness model with the normal distribution law

- For surfaces with an irregular character, the ordinates distribution does not comply with the normal distribution law according to the 3D asymmetry *Ssk*; the deviation reaches 100 %.
- For surfaces with an irregular character, the ordinates distribution complies with the normal distribution law according to the 3D kurtosis *Sku*; the maximum deviation is 13 %.
- The values of the roughness parameters *Rsk* and *Rku* of the X-axis and Y-axis profiles coincide with *Ssk* and *Sku* only for isotropic surfaces; for anisotropic ones, in the Y-axis direction, the deviations from the 3D values reach 100 %.
- At an increased evaluation length of Y-axis profiles, the asymmetry *Rsk* and kurtosis *Rku* of the ordinates distribution correspond to the 3D roughness values.

Results regarding the surface arithmetic mean height *Sa*

- For mathematical determination and prediction of the roughness parameter *Sa,* Expression (3.3), which includes the kurtosis value of the ordinates distribution function, has to be used. The difference between the calculated and experimentally determined *Sa* values is less than 1 %.
- The values of the parameter *Ra* in direction perpendicular to the machining traces have a minimal deviation from the value of the 3D parameter *Sa* (up to 5 %), which confirms the coincidence of the mutual location of the mean lines of the X-axis profiles and the mean plane after leveling line by line + LS-polynomial.
- The values of the parameter *Ra* in the direction parallel to the machining traces have significant deviations from the value of the 3D parameter *Sa* (up to 34 %), which can be explained by the displacement between the mean lines of the Y-axis profiles and the surface mean plane.

Results regarding surface anisotropy

- The surface texture aspect ratio *Str* of the standard ISO 25178-2 corresponds to the anisotropy coefficient *C* and expresses the ratio between the roughness steps perpendicular to and parallel to the machining traces.

Results regarding the surface roughness step *RSm_2*

- To determine the surface roughness step in the direction parallel to the machining traces, the waviness step value WSm_2 at the threshold $H = 1\ 0\%$ should be used.
- When determining the parameter WSm_2, a cut-off should be selected which is one unit smaller than the standardized one (depending on the value of the parameter *Sa*).
- When determining the value of average roughness step RSm_2' for profiles taken at $L = 5l$, the correction coefficient $k_{pr} = 1.16$ should be used.

Results regarding the material volume *Vm*

- For mathematical determination and prediction of the material volume *Vm',* Equation (3.14) should be used.
- The experimentally determined values of the material volume *Vm'* at $\gamma > 1$ are smaller than the theoretical ones, which could be explained by the insufficient evaluation area of the sample surface, which will be checked in Chapter 5.

4. PRECISION OF DETERMINATION OF ROUGHNESS PARAMETERS

The practical application of roughness parameters requires their accurate determination experimentally. The measurement accuracy of surface roughness is related to the determination of the dimensions of the surface evaluation area. In practice, the evaluation area is limited by the dimensions of the sample and the specification of the measuring equipment; therefore, it is necessary to determine the optimal evaluation area and the required number of experiments that would ensure sufficient accuracy for performing engineering calculations. In engineering calculations, the permissible relative error ε should not be greater than 0.1, and the confidence level β is usually in the range of 0.8–0.95. Accordingly, in this Thesis, the measurement accuracy of roughness parameters was determined at ε = 0.1 and β = 0.9.

4.1. Arithmetic mean height *Sa*

The required number of measurements for the accurate determination of the parameter *Sa* is calculated as follows [36]:

$$n_{Sa} = \frac{t_{\beta^2} \times \pi}{4 \times \varepsilon^2 \times Str \times \alpha_1 \times Aa}, \tag{4.1}$$

where α_1 is the approximation parameter of the correlation function in the direction perpendicular to the machining traces.

Graphs in Fig. 4.1 reflect the values of the number of measurements for the parameter *Sa* depending on the evaluation length *L* (or the length of the edge of the evaluation area) for anisotropic surfaces. Each graph has 5 sections that correspond to the size of the evaluation length *L*, which includes 1, 2, 3, 4 or 5 section lengths l_{sc}. Depending on the *Sa* value, the section length value changes in accordance with the data of the Standard ISO 21920-2. From the graph, it can be concluded that for very smooth surfaces, with *Sa* < 0.05 µm, the minimum evaluation length *L* should be equal to two section lengths to achieve the required accuracy within one measurement. For surfaces with *Sa* > 0.05 µm, accurate measurements at $n_{Sa} = 1$ will be achieved by choosing the evaluation area with an edge equal to one section length.

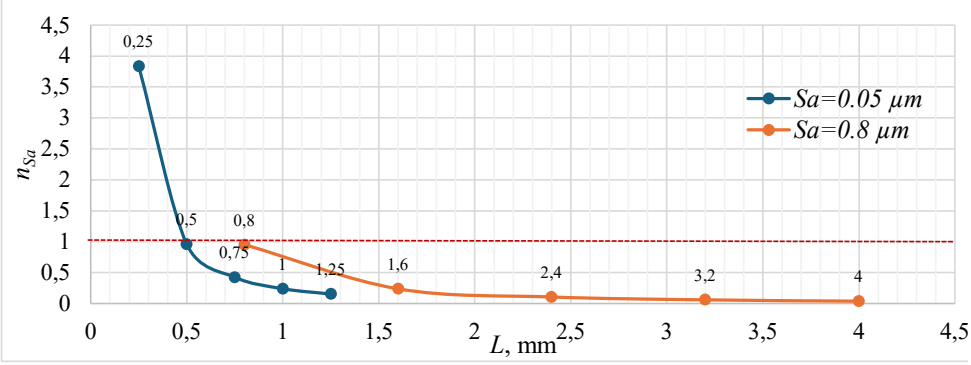

Fig. 4.1. Number of measurements for the parameter *Sa* depending on the evaluation length *L* for anisotropic surfaces. ε = 0.1; β = 0.9.

4.2. Mean roughness profile element spacing *RSm*

The required number of measurements to determine the parameter *RSm* is calculated according to the formula:

$$n_{RSm} = \frac{t_{\beta^2}\pi\sqrt{\pi}}{4 \times \varepsilon^2 \times L\sqrt{\alpha}}. \quad (4.2)$$

The results of calculating the determination accuracy of the roughness parameter *RSm* in the X-axis and Y-axis directions at $\varepsilon = 0.1$ and $\beta = 0.9$ are presented in Table 4.1. The $N(0)$ values, determined from the profilograms, once again prove that the smaller the *Sa* values, the finer the roughness step and, accordingly, the greater the number of profile intersections with the mean line along the evaluation length. In the direction perpendicular to the machining traces, the number of $N(0)$ is approximately 30 times greater than in the direction parallel to the machining traces, which characterizes the anisotropy of the ground surfaces.

Table 4.1

The Required Number of Measurements for Determining the Parameter *RSm* for Ground Surfaces at $\varepsilon = 0.1$ and $\beta = 0.9$

Specimen	*Sa, μm*	*Direction*	*l, mm*	*L, mm*	*N(0)*	α, mm^{-2}	n_{RSm}	$L_{for\ a\ single\ measurement}$, *mm*
Rugotest 104, N1	**0.025**	**X**	**0.25**	1.25	150	70989	2	1.41
		Y			5	79	34	42.28
Rugotest 104, N2	**0.05**	**X**	**0.25**	1.25	175	96624	1	1.21
		Y			5	79	34	42.28
Rugotest 104, N4	**0.2**	**X**	**0.8**	4	136	5699	2	4.97
		Y			4	4.9	43	169.12
Rugotest 104, N6	**0.8**	**X**	**0.8**	4	130	5207	2	5.20
		Y			4	4.9	43	169.12
Rugotest 104, N8	**3.2**	**X**	**2.5**	12,5	185	1079	1	11.5
		Y			6	1.13	29	352.33

According to the results of the calculation of determination accuracy of the *RSm* parameter, it can be concluded that in the direction perpendicular to the machining traces, it is necessary to perform 1–2 2D profile measurements, but in the Y-axis direction – more than 30 measurements, to obtain reliable *RSm* values at the evaluation length $L = 5l$. When performing one measurement experiment in the direction parallel to the processing traces at the given $\varepsilon = 0.1$ and $\beta = 0.9$, a significantly large evaluation length is required. Still, not in all cases the sample dimensions are sufficient to take a long profilogram.

In the case of 3D roughness measurements, several profiles are taken within one experiment; theoretically, additional experiments are not required to ensure the accuracy of RSm_2. The number of profiles in the X-axis direction is several thousand, and in the Y-axis direction, several hundred. It means that one 3D roughness measurement experiment includes the calculated n_{Rsm} for the profile.

4.3. Material volume *Vm*

The following relationship was used to determine the required number of measurements n_{Vm} of the material volume *Vm*:

$$n_{Vm} = \frac{t_\beta^2 \times 2\pi \times \left([1 - \Phi(\gamma)]^2 + \sum_{i=2}^{\infty} \frac{1}{i^2 i!} \left[\Phi^{(i-1)}(\gamma) \right]^2 \right)}{\varepsilon^2 \times L^2 \times Str \times \alpha_1 \times \left\{ \frac{1}{\sqrt{2\pi}} e^{-\frac{\gamma^2}{2}} - \gamma[1 - \Phi(\gamma)] \right\}^2}. \quad (4.3)$$

Table 4.2 shows the necessary data for determination of n_{Vm} of the ground surface at $\varepsilon = 0.1$ and $\beta = 0.9$ depending on the relative deformation level γ and the evaluation length *L*.

Table 4.2

The Required Number of Measurements for Determination of the Parameter *Vm* at Different Relative Deformation Levels

No.	*L*	*Str*	$N_1(0)$	α_1	γ	n_{Vm}
1.	0.25	0.025	34	91181.6	**1**	144
2.	0.5		68	91181.6		36
3.	0.75		102	91181.6		16
4.	1		136	91181.6		9
5.	1.25		170	91181.6		6

No.	*L*	*Str*	$N_1(0)$	α_1	γ	n_{Vm}
1.	0.25	0.025	34	91181.6	**2**	482
2.	0.5		68	91181.6		120
3.	0.75		102	91181.6		54
4.	1		136	91181.6		30
5.	1.25		170	91181.6		19

No.	*L*	*Str*	$N_1(0)$	α_1	γ	n_{Vm}
1.	0.25	0.025	34	91181.6	**3**	1660
2.	0.5		68	91181.6		412
3.	0.75		102	91181.6		185
4.	1		136	91181.6		103
5.	1.25		170	91181.6		65

According to the data in Table 4.2, it can be concluded that for the accurate determination of the material volume *Vm*, even at standardized size of evaluation area, several separate 3D roughness measurements must be performed. In addition, as the deformation level increases, the volume of measurement experiments increases several times. This is evidence of why the experimental values of the parameter *Vm* in Section 3.5 had significant deviations from the calculated ones.

4.4. Conclusions

- The accuracy of determination of the roughness parameters *Sa*, RSm_1 and RSm_2 at a relative error of 0.1 and a confidence level of 0.9 will be ensured by performing one 3D roughness measurement at a standardized evaluation length, which consists of 5 section lengths.
- To ensure the accuracy of the determination of material volume *Vm* at a relative error of 0.1 and a confidence level of 0.9, from 6 to 65 3D roughness measurements have to be performed, depending on the relative deformation level.

4.5. Recommendations for the determination of the roughness parameters

The developed recommendations are suitable for complex experimental and analytical determination of the roughness parameters *Sa*, RSm_1, RSm_2, *Str*, and *Vm* for surfaces with an irregular roughness and pronounced anisotropy.

1. Before a 3D surface roughness measurement:
   1.1. Choose the size of the edge of the evaluation area (square) that would correspond to 5 section lengths. The section length is chosen depending on the previously determined or already known *Ra*/*Sa* value according to the standard ISO 21920 data.
   1.2. Depending on the dimensions of the evaluation area, choose the appropriate distance between the surface points along the X and Y axes and the number of points, taking into account the specification of the measuring device and the limitation of the measurement experiment (e.g., the maximum number of points).
   1.3. Ensure that the topography is taken in a direction perpendicular to the machining traces. If the sample dimensions are less than 5 section lengths, additional experiments must be performed according to the equations in Chapter 4.
2. After a 3D roughness measurement:
   2.1. Perform surface leveling using the leveling line-by-line function together with a 1st or 2nd order polynomial.
   2.2. To determine the parameter *Sa*, the appropriate computer operation "Calculate" should be selected.
   2.3. The parameter *RSm* is determined between all profiles in the X-axis and Y-axis directions, using the function "Extract all profiles" and selecting the relevant profile direction.
   2.4. To determine the parameter RSm_1 for all X-axis profiles, use the computer operation "Calculate" → standard ISO 21920→ and a threshold of 10 %.
   2.5. There are two options for the determination of the parameter RSm_2:
      2.5.1. The parameter RSm_2 is determined using the surface texture aspect ratio *Str* according to Equation (3.10).
      2.5.2. Extract all Y-axis profiles from the leveled surface. Using the computer program function "Calculate" → standard ISO 21920, select the "Waviness" profile with a cut-off one unit smaller than the sampling length → threshold 10 %. Calculate RSm_2' using the correction coefficient k_{pr} according to Equation (3.1).
   2.6. To determine the parameter *Str*, select the appropriate computer operation "Calculate".
   2.7. To determine the parameter *Vm* at a specific relative deformation level, select the function "Slices". Entering the required level: 1*Sq*, 2*Sq*, etc., read the "Volume of material" value.

5. DETERMINATION OF WEAR INTENSITY AND LINEAR WEAR

In this Thesis, the analysis of the process of surfaces contacting and wear resistance was performed with the assumption that one surface is completely smooth and hard, which eliminates the necessity to determine the probability of surface contact, which leads to complex calculations. According to [6], the wear intensity I_h is determined by the equation:

$$I_h = \frac{V'}{n \times d \times Aa'}, \tag{5.1}$$

where

V' – volume of deformed material, mm^3;
n – number of cycles to failure;
d – contact length, mm.

At the beginning of solving engineering tasks, it is important to determine how the microirregularities of the surface will deform, mainly elastically or plastically. The contact area, to a greater extent, is characterized by the ability of the surface microirregularities to deform elastically, which can be described by the contact type criterion KK [37]:

$$KK = \frac{RSm_1 \times \theta \times H}{Sa}, \tag{5.2}$$

where θ is the elastic constant of the material, MPa^{-1}, and H is the hardness, MPa.

The elastic constant of the material is calculated by the formula:

$$\theta = \frac{1 - \mu_2^2}{\pi \times E_2}, \tag{5.3}$$

where μ is Poisson's ratio, and E is the elastic modulus, MPa.

If the value of the contact type criterion is ≥ 1.74, then the condition of elastic deformation is fulfilled, but if $KK \leq 0.7$, the contact is plastic.

Determination of the wear intensity according to Equation (5.1) also requires the study of the contact size, which can be expressed as the length of the real contact area d in the friction direction [57]:

$$d = RSm[1 - \Phi(\gamma)]e^{\frac{\gamma^2}{2}}. \tag{5.4}$$

The relative deformation level γ and the number of cycles to material failure are determined depending on the contact type – elastic or plastic.

Analyzing Equation (5.1), it can be concluded that there is no need to look for the exact value of the volume of deformed material, since V' in any case will be corrected by the semi-empirical value n – the number of cycles to material failure. Therefore, instead of the parameter V', the parameter Vm of the standard ISO 25178-2 (using the function "Slices"), determined at the specific relative deformation level, can be used.

5.1. Wear calculation in the case of elastic contact

After defining the type of elastic contact, the next step is the determination of the relative deformation level γ:

$$F_1(\gamma) = \left(\frac{q_{el} \times \theta_{sum}}{k_{el}}\right) \times \left(\frac{RSm_1}{Sa}\right), \tag{5.5}$$

where

$F_1(\gamma)$ – tabulated function [37];

q_{el} – load, MPa;

k_{el} – coefficient that depends on the anisotropy of the surface [37];

θ_{sum} – total elastic constant of material, MPa^{-1}.

The total elastic constant is calculated taking into account the physical-mechanical characteristics of both contacting parts:

$$\theta_{sum} = \frac{1 - \mu_1^2}{\pi \times E_1} + \frac{1 - \mu_2^2}{\pi \times E_2}. \tag{5.6}$$

The calculated value of the function $F_1(\gamma)$ determines the deformation level γ [37]. The number of cycles to material failure after some transformations can be expressed by the following equation [6]:

$$n_{el} = \left(\frac{3\theta\sigma_0}{4kf\sqrt{2\pi(4\gamma - \gamma^2)}} \times \frac{RSm_2}{Sa}\right)^{t_{el}}, \tag{5.7}$$

where

k – constant, depending on friction-fatigue characteristics [6];

f – coefficient of friction;

σ_0 – limit of durability of the material, MPa;

t_{el} – fatigue curve parameter [6].

The wear intensity in the case of elastic contact is proposed to be calculated according to the following formula:

$$I_{h\_el} = \frac{V_m}{\left(\frac{3\theta\sigma_0}{4kf\sqrt{2\pi(4\gamma - \gamma^2)}} \times \frac{RSm_2}{Sa}\right)^{t_{el}} \times RSm_2[1 - \Phi(\gamma)]e^{\frac{\gamma^2}{2}} \times Aa}. \tag{5.8}$$

According to Equation (5.8), it can be concluded that changes in the friction coefficient lead to significant changes in the wear intensity, especially if $f = 0.2 \ldots 0.3$. Wear increases with an increase in the elastic modulus. With an increase in the values of Poisson's ratio μ, the wear intensity decreases. An increase in the value of the parameter σ_0 reduces the wear value, the larger the fatigue curve parameter t is. The wear intensity depends on the arithmetic mean height Sa and the roughness steps RSm_1 and RSm_2. The analysis indicates that by reducing the Sa value and increasing the RSm value, the wear intensity reduces, because in this case, the surface microirregularities have a sloping character.

5.2. Wear calculation in the case of plastic contact

In the case of plastic contact, the relative deformation level γ is determined by the calculated value of the function $F_2(\gamma)$:

$$F_2(\gamma) = \frac{q_{plast.}}{H \times k_{plast}}, \tag{5.9}$$

where

$F_2(\gamma)$ – tabulated function [37];
q_{plast} – load, MPa;
k_{plast} – coefficient that depends on the anisotropy of the surface [37].

The calculated value of the function $F_2(\gamma)$ determines the deformation level γ [37]. The number of cycles to material failure in the given case is expressed by the following Equation [6]:

$$n_{plast} = \left(\frac{e_0}{2\pi} \sqrt{\frac{\sigma_T - 2fH}{\sigma_T + 2fH}} \times \frac{1}{\pi(4\gamma - \gamma^2)} \times \frac{RSm_2}{Sa} \right)^{t_{plast}}, \tag{5.10}$$

where σ_T is the material yield strength, MPa, and t_{plast} is a fatigue curve parameter [6].

The wear intensity in the case of plastic contact is proposed to be calculated by the following formula:

$$I_{h\_plast} = \frac{V_m}{\left(\frac{e_0}{2\pi} \sqrt{\frac{\sigma_T - 2fH}{\sigma_T + 2fH}} \times \frac{1}{\pi(4\gamma - \gamma^2)} \frac{RSm_2}{Sa} \right)^{t_{plast}} \times RSm_2 [1 - \Phi(\gamma)] e^{\frac{\gamma^2}{2}} \times Aa}. \tag{5.11}$$

The linear wear value h is expressed by the following equation:

$$h = J_h \times L_{ber}, \tag{5.12}$$

where L_{ber} is the friction path, mm.

$$L_{ber} = V \times t, \tag{5.13}$$

where V is the rotation speed, m/s, and t is working time, s.

So, in the case of plastic contact, the friction coefficient f has a significant effect. At a friction coefficient $f > 0.2$, there is a rapid increase in wear intensity. In addition, as the value of the parameter σ_T increases, the wear intensity decreases. As the hardness H increases and the load q decreases, the wear intensity also decreases. The sensitivity of the wear value to the *Sa/RSm* ratio is lower in comparison with elastic contact, which can be explained by an additional link between the surface roughness parameters and the relative deformation level γ. In the case of elastic contact, the roughness parameters have a greater effect on the deformation level.

It is quite important to compare the influence of various parameters on the wear intensity by determining its specific weight. For this purpose, relationships were constructed that reflect the influence of various parameters on the wear intensity in the cases of elastic and plastic contact, which can be seen in Fig. 5.1 a, b. They show changes in the parameter values and the corresponding increase of I_h.

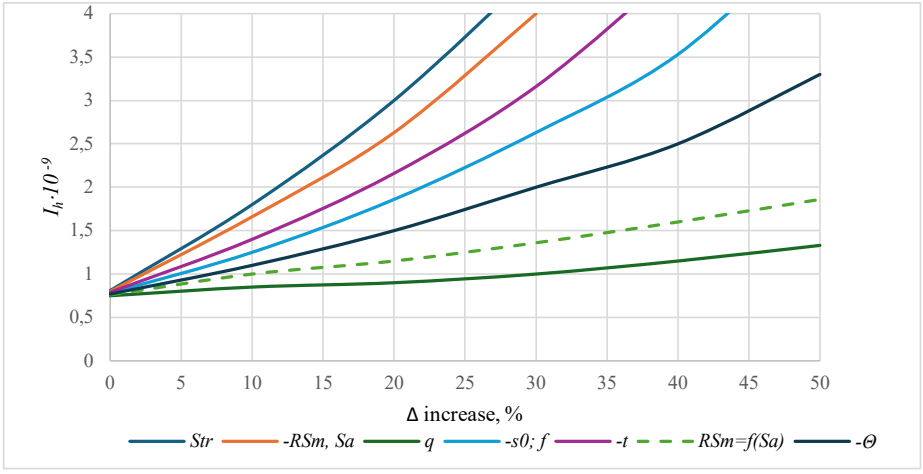

a

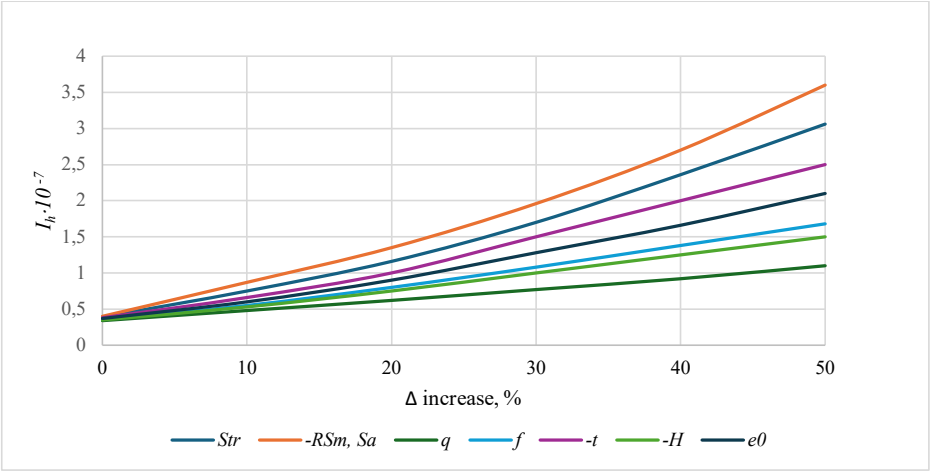

b

Fig. 5.1. The influence of parameter changes on the wear intensity I_h:
a – in the case of elastic contact; b – in the case of plastic contact.

If we assume that the values of the parameters affecting wear change independently of each other, we can conclude that the wear intensity is most influenced by the roughness parameters. Such results can be explained by the existence of a correlation between individual parameters. Such a link exists for the parameters *Sa* and *RSm*, *Sa, f,* etc. The roughness parameters *Sa* and *RSm* have the same but opposite influence on the change in I_h, which means that to increase the wear resistance, it is necessary to reduce the height of the micro-irregularities *Sa* or increase the roughness step *RSm*.

5.3. Comparison of analytical calculation results and friction experiment data

To verify the correctness of the wear determination model, it is necessary to compare the analytical calculation results with experimental data. For this purpose, testing of the friction pair steel (102Cr6)-bronze (CW307G) was carried out on the CSM Instruments tribometer according to the pin-on-disk scheme [17]. The friction experiment scheme and the necessary equipment are shown in Fig. 5.2. The pin surface was polished before the friction experiment to ensure a constant nominal contact area between the pin surface and the rotating disk.

a b

Fig. 5.2. Representation of the friction experiment:
a – CSM Instruments tribometer; b – testing according to the scheme pin (2) on disk (1).

To determine the linear wear, five experiments were performed at the disk rotation speed $v = 0.3$ m/s and the applied load $q = 1.45$ MPa, and the average value was calculated. To determine the linear wear, it was necessary to explore the tribotrack cross-sectional area. For this purpose, measurements of tribotrack profiles were performed in four places, using the computer program McubeMapUltimate 10.

The next step was the calculation of the wear intensity and linear wear of the steel-bronze friction pair. Wear was analytically determined for the bronze disk after the running-in stage. The constructive characteristics correspond to the settings of the friction experiment. The values of the roughness parameters *Sa*, *Str, RSm*$_1$, and *RSm*$_2$ correspond to experimentally determined values after the running-in stage. Physical-mechanical and friction-fatigue characteristics were determined according to material standards and manuals.

1) The elastic constant of the material was determined:

$$\theta = \frac{1-0.34^2}{1.15\cdot 10^5} = 0.24 \times 10^{-5}(\text{MPa}^{-1}).$$

2) Accordingly, the contact type criterion *KK*:

$$KK = \frac{0.035\cdot 0.24\cdot 10^{-5}\cdot 200}{1.7\cdot 10^{-3}} = 0.01.$$

We assume that in this case, plastic contact is provided ($KK \leq 0.7$).

3) The relative deformation level γ in the case of plastic contact was determined as follows:

$$F_2\{\gamma\} = \frac{1.45}{200 \cdot 1.147^*} = 0.63 \cdot 10^{-2}.$$

*k_{plast} = 1.147 is the tabulated value, obtained at *Str* = 0.03.

In this case, the calculated level γ = 2.5.

3) The number of cycles to material failure:

$$n_{plast} = \left(\frac{0.39}{2\pi} \sqrt{\frac{360 - 2 \times 0.18 \times 200}{360 + 2 \times 0.18 \times 200}} \times \frac{1}{\pi(4 \times 2.5 - 2.5^2)} \cdot \frac{1.16}{1.7 \times 10^{-3}} \right)^2 = 4699.$$

4) The length of the contact area:

$$d = 1.16 \times [1 - \Phi(2.5)] e^{\frac{2.5^2}{2}} = 0.135(\text{mm}).$$

5) The volume of the deformed material:

$$Vm = 3.46 \times 2,.5 \times 10^{-3} \times \left\{ \frac{1}{\sqrt{2\pi}} e^{-\frac{2.5^2}{2}} - 2.5[1 - \Phi(2.5)] \right\} = 1,.9 \times 10^{-5}(\text{mm}^3).$$

6) The wear intensity:

$$I_h = \frac{1.49 \times 10^{-5}}{4699 \times 3.46 \times 0.135} = 5.62 \times 10^{-9}.$$

7) The friction path was determined by the rotation speed and working time:

$$L_{tr} = 0.3 \times 13334 = 4000 \text{ (m)}.$$

8) Linear wear:

$$h = 5.62 \times 10^{-9} \times 4000 \times 10^6 = 22.48 \text{ (μm)}.$$

The experimentally determined and calculated values of linear wear for specific friction paths are reflected in Table 5.1.

Table 5.1

Experimental and Calculated Values of Linear Wear

Type of value	**Value of a linear wear, μm**							
	After 500 m	**After 1000 m**	**After 1500 m**	**After 2000 m**	**After 2500 m**	**After 3000 m**	**After 3500 m**	**After 4000 m**
Theoretical	2.92	5.62	8.43	11.24	14.05	16.86	19.67	22.48
Experimental	3.07	5.75	8.41	11.22	13.53	16.67	18.74	21.33
Relative deviation, %	**–4.88**	**–2.26**	**0.24**	**0.18**	**3.84**	**1.14**	**4.96**	**4.95**

Comparing experimental data with calculation results, it can be concluded that the difference between the values is on average 5 %, which is a good justification for the high accuracy of calculations based on the proposed wear calculation model.

5.4. Conclusions

1. The relative deviation between the results of the analytical calculation of wear and the results of the experiment does not exceed 5 %.
2. Increment in the *Sa/RSm* ratio gives an increase in wear intensity.
3. For the correct determination and prediction of wear intensity, the correlation between the roughness parameters *Sa* and *RSm* should be taken into account.
4. The smaller the surface anisotropy (the larger the *Str* value), the greater its effect on wear intensity.
5. To increase wear resistance, the main attention should be paid to the selection of the material of the parts of the friction pair, but to reduce the running-in time, to the roughness parameters of the friction surfaces, so that the minimum *Sa/RSm* ratio is ensured.

5.5. Wear determination methodology

The proposed methodology is suitable for the determination of wear intensity and linear wear for flat friction surfaces with irregular roughness, if fatigue failure of the material surface occurs. The calculation of wear intensity is performed in the following order:

1. Determine the initial data:
   1.1. Micro-geometric parameters of the friction surfaces: $Sa, RSm_1, RSm_2, Str, Vm;$
   1.2. Physical and mechanical characteristics of the material surface layer: $H, E, \mu, f, \sigma_T;$
   1.3. Fatigue characteristics of the material: $\sigma_0, e_0, t;$
   1.4. Constructive characteristics: $Aa, q, L_b.$
   - The geometry of the friction surfaces is determined by performing a measuring experiment on a profilograph-profilometer. The roughness parameters are determined according the recommendations in Section 4.5. In the case of wear prediction, values of *Sa* and *Vm* are determined analytically, changing the value of *Sq*.
   - The physical-mechanical and fatigue characteristics of the material are determined according to the results of mechanical tests and technical manuals.
   - Constructive parameters are determined according to the drawing of the friction pair and the set operating conditions.
2. Calculate the elastic constant of the material θ for the wearing part and the total elastic constant of material θ_{sum} for both friction surfaces.
3. Determine the contact type criterion *KK*.
4. Determine the relative deformation level γ depending on the type of *KK*.
5. Calculate wear intensity and the linear wear for the corresponding contact type.

Figure 5.3 shows the wear intensity and linear wear calculation scheme, taking into account the contact type criterion.

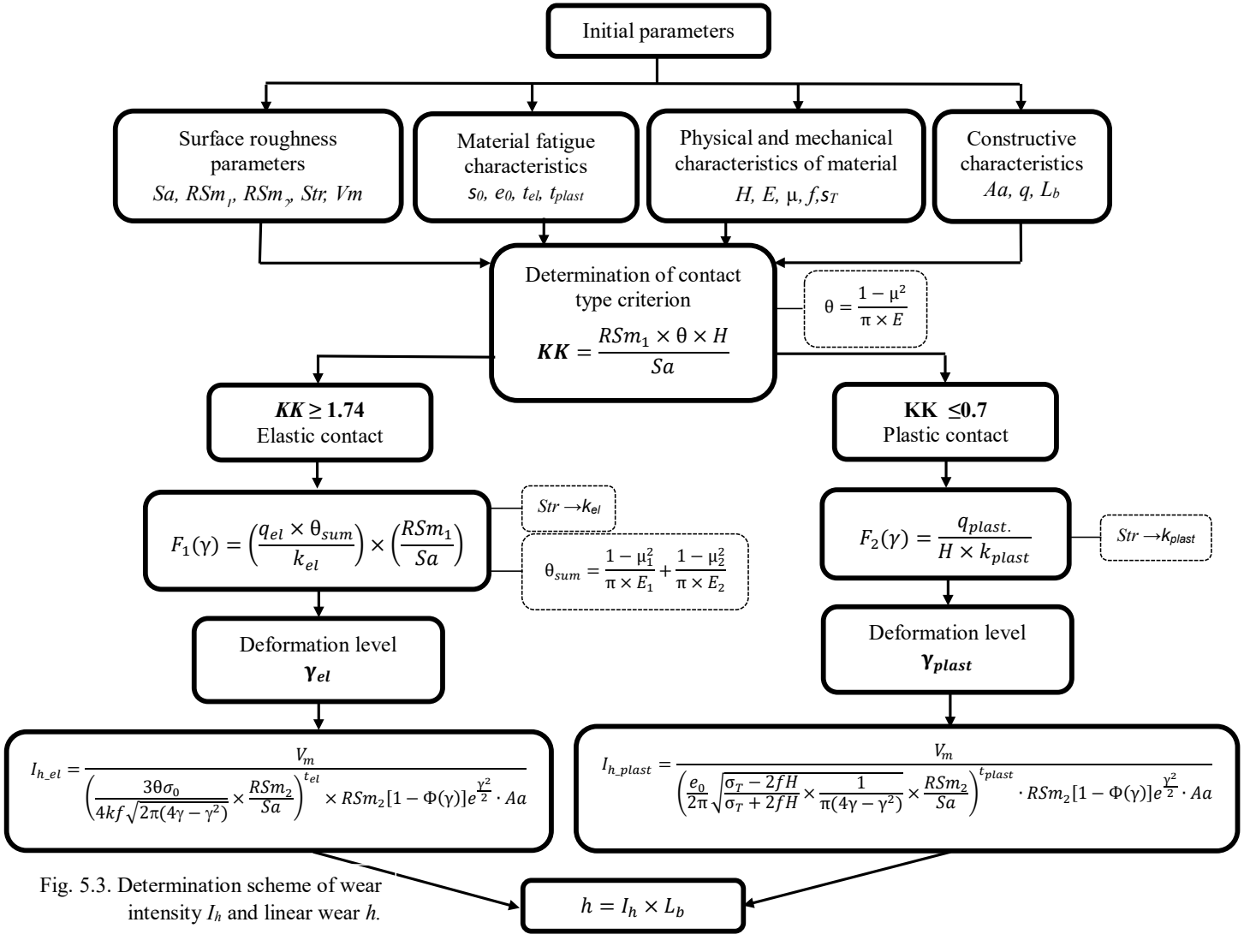

Fig. 5.3. Determination scheme of wear intensity I_h and linear wear h.

MAIN RESULTS AND CONCLUSIONS OF THE THESIS

Today, several wear determination models have their own limitations: 2D roughness parameters, the assumption of the normality of the ordinates distribution, as well as one specific type of contact. When performing wear simulation and calculation in a finite element environment, in several cases, researchers use Archard and Fleischer wear calculation models, and a simplified contact model of a friction pair (smooth surface-smooth surface), where surface roughness is not taken into account, which accordingly reduces the reliability of the results. In the existing wear calculation models, the correctness of the application of roughness parameters and the accuracy of their determination are not justified, which also reduces the reliability of the obtained results. To solve the existing problem, the following hypothesis was advanced: The specified determination and integration of the 3D and 2D surface roughness parameters, as well as the use of individual material fatigue characteristics in wear intensity calculations and prediction, will increase the reliability of the results for elastic and plastic contact cases. Confirmation of this hypothesis is visible in the following achieved results:

1. Because the type of leveling affects the roughness geometry, the mutual arrangement of the surface mean plane and profiles' mean lines, the optimal 3D leveling method for preservation of the geometry of the surface profiles was chosen – leveling line by line together with 1st/2nd order LS-polynomial.
2. For surfaces with an irregular roughness, the distribution of ordinates is close to normal, but does not completely correspond to it according to the experimental values of 3D asymmetry and kurtosis criteria *Ssk* and *Sku*; in turn, it doesn't have a strong influence on the analytical determination of the arithmetic mean height *Sa*. However, to increase the accuracy of the results, it was proposed to calculate the parameter *Sa*, taking into account the *Sku* value.
3. It was proven that the surface texture aspect ratio *Str* from the standard ISO 25178-2 complies with the anisotropy coefficient; respectively, it can be used for the determination of the roughness step RSm_2, which is complicated by the deviation between the surface mean plane and the profiles' mean lines.
4. The accuracy of determination of the roughness parameters *Sa*, RSm_1, and RSm_2 at a relative error of 0.1 and a confidence level of 0.9 will be ensured by one 3D roughness measurement at the standardized evaluation length.
5. For the experimental determination of the volume of deformed material *Vm* at relative deformation levels $\gamma > 1$, a series of additional measurements must be performed to ensure the accuracy of the determination of the given parameter. The parameter *Vm* values obtained within the one measurement experiment are less than the calculated ones.
6. Within the Doctoral Thesis, the methodology for the determination of the roughness parameters *Sa*, RSm_1, RSm_2, and *Vm* was developed, considering the specific character of surfaces with irregular roughness.

7. The results of the analytical calculations of linear wear by the developed model give a high congruence with the results of the friction experiment in the case of plastic contact; the relative deviation is 5 %.
8. Within the Doctoral Thesis, the methodology for the determination of the wear intensity and the linear wear for flat friction surfaces with irregular roughness, if fatigue failure of the material surface occurs, was developed.
9. For the correct determination and prediction of the wear intensity, the correlation between the roughness parameters *Sa* and *RSm* should be taken into account. Increasing the *Sa/RSm* ratio increases the wear intensity.

RECOMMENDATIONS FOR FURTHER RESEARCH

1. To check the compliance of the wear determination model with experimental data in the case of elastic contact.
2. To perform wear intensity calculations in the finite element environment (FEM) and compare the obtained results with experimental data.

BIBLIOGRAPHY

1. Johnson K. L. *Contact Mechanics*. Cambridge Univ. Press, 1985, 452 p.
2. Lockrey A. *An evaluation of adhesive contact models for elastic solids using atomic force microscopy.* University of Southampton, United Kingdom, 2021, 43 p.
3. Bowden F. P.; Tabor D. *The friction and lubrication of solids*. Oxford at the Clarendon press, 1950, 331 p.
4. Archard J. F. *Elastic deformation and the laws of friction*. Proceedings of the Royal Society of London. Series A, Mathematical and Physical Sciences, vol. 243, no. 1233, 1957, pp. 190–205.
5. Popova, E.; Popov, V. L.; Kim, D.E. *60 years of Rabinowicz' criterion for adhesive wear.* Friction, vol.6, 2018 , pp. 341–348.
6. Kragelsky, I. V.; Alisin, V. V. *Tribology: Lubrication, Friction and Wear*. UK: Professional Engineering Publishing limited London and Bury St Edmunds, 2005, 948 p.
7. Fleischer, G; Gröger, H.; Thum, H. *Verschleiß und Zuverlässigkeit, 1st ed.;* Verlag Technik: Berlin, Germany, 1980, 244 p.
8. Chun, S. M.; Khonsari, M. M. *Wear simulation for the journal bearings operating under aligned shaft and steady load during start-up and coast-down conditions*. Tribol. Int., vol. 97, 2016, pp. 440–466.
9. Lijesh, K. P.; Khonsari, M. M. *On the Modeling of Adhesive Wear with Consideration of Loading Sequence*. Tribol. Lett., vol. 66, iss. 3, 2018, art. no. 105.
10. Lijesh, K.; Khonsari, M.; Kailas, S. V. *On the integrated degradation coefficient for adhesive wear: A thermodynamic approach*. Wear, vol. 408–409, 2018, pp.138–150.
11. Xiang, G.; Han, Y.; Wang, J.; Wang, J.; Ni, X. *Coupling transient mixed lubrication and wear for journal bearing modeling.* Tribol. Int., vol. 138, 2019, pp. 1–15.
12. Xiang, G.; Yang, T.; Guo, J.; Wang, J.; Liu, B.; Chen, S. *Optimization transient wear and contact performances of water-lubricated bearings under fluid-solid-thermal coupling condition using profile modification*. Wear, vol. 502-503, 2022, art. no. 204379.
13. Lehmann, B.; Trompetter, P.;Guzmán, F. G.; Jacobs, G. *Evaluation of Wear Models for the Wear Calculation of Journal Bearings for Planetary Gears in Wind Turbines*. Lubricants, vol. 11, iss. 9, 2023, art. no. 364.
14. Greenwood, J. A.; Williamson, J. P., 1966. *Contact of nominally flat surfaces*. Proceedings of the royal society of London. Series A. Mathematical and physical sciences, vol. 295, 1966, pp. 300–319.
15. Рудзит Я. А. *Микрогеометрия и контактное взаимодействие поверхностей.* Рига, Зинатне, 1975, 211 стр. (in Russian).
16. Konrads G. *Mašīnu detaļu slīdes virsmu dilšana*. – Rīga, RTU Izdevniecība, 2006. 80 lpp. (in Latvian)
17. Spriņģis G. *Slīdes berzes pāra detaļu nodiluma analīze un noteikšana*. Promocijas darbs. Rīga: RTU Izdevniecība, 2023. 101 lpp. (in Latvian)

18. Youngbin L., Sangyul H. *RufGen: A plug-in for rough surface generation in Abaqus/CAE.* SoftwareX 22, 2023.
19. David Bergström. *Rough surface generation & analysis* [online]. [25.08.2025] Available from: https://www.mysimlabs.com/surface_generation.html.
20. Yan L., Guan L., Wang D., Xiang D. *Application and prospect of wear simulation based on ABAQUS: A Review*. Lubricants, Vol. 12, art. no. 57, 2024, pp. 1–26.
21. Fallahnezhad, K.; Oskouei, R. H.; Taylor, M. *Development of a fretting corrosion model for metallic interfaces using adaptive finite element analysis*. Finite Elem. Anal. Des. 2018, vol. 148, pp. 38–47.
22. Gan, L.; Xiao, K.; Pu, W.; Tang, T.; Wang, J. X. *A numerical method to investigate the effect of thermal and plastic behaviors on the evolution of sliding wear*. Meccanica, vol.56, 2021, pp. 2339–2356.
23. Shen, F.; Hu, W.; Meng, Q. *A damage mechanics approach to fretting fatigue life prediction with consideration of elastic-plastic damage model and wear*. Tribol. Int. 2015, 82, 176–190.
24. Duo, Yang, et al. *Discrimination of Wear Performance Based on Surface Roughness Parameters Arithmetic Mean Height (Sa) and Skewness (Ssk)*. Wear, vol. 548–549, 2024, p. 1–10.
25. Hao, Q.; Yin, J.; Liu, Y.; Jin, L.; Zhang, S.; Sha, Z. *Time-Varying Wear Calculation Method for Fractal Rough Surfaces of Friction Pairs*. Coatings, vol.13, iss.2, 2023, art. no.270.
26. Li L., Li G. H., Wang J. J., Fan C. Q., Cai A. J. *Fretting wear mechanical analysis of double rough surfaces based on energy method*. Proceedings of the Institution of Mechanical Engineers, Part J: Journal of Engineering Tribology, vol. 237, iss. 2, 2023, pp. 356–368.
27. Awwad K., Fallahnezhad K., Yousif BF., et al. *Finite element analysis and experimental validation of polymer–metal contacts in block-on-ring configuration*. Friction, vol.12, iss. 3, 2023, pp. 554–568.
28. Maier M., Pusterhofer M., Grün F. *Modelling Approaches of Wear-Based Surface Development and Their Experimental Validation*. Lubricants, vol. 10, iss.10, 2022, art. no. 335.
29. Tandler R., Bohn N., Gabbert U., Woschke E. *Analytical wear model and its application for the wear simulation in automotive bush chain drive systems*. Wear, vol. 446–447, 2020, art. no. 203193.
30. Ting, Chen; Weiguo, Ma; Kaihui, Zhu; Zilong, Hu. *Wear simulation of UHMWPE against the different counterface roughness in reciprocating unidirectional sliding motion*. Scientific reports, vol.14, iss.1, 2024, art. no.15858.
31. Bose, K.; Ramkumar, P. *Finite Element Sliding Wear Simulation of 2D Steel-on-Steel Pin-on-Disc Tribometer.* SAE Technical Paper 2018-28-0011, 2018.
32. Li, C., Karimbaev, R., Wang, S., Amanov, A., Wang, D., Abdel Wahab, M. *Fretting Wear Behavior of Inconel 718 Alloy Manufactured by DED and Treated by UNSM.* Sci. Rep., vol.13, iss.1, 2023, art. no. 1308.
33. Terwey, J. T.; Fourati, M. A.; Pape, F.; Poll, G. *Energy-Based Modelling of Adhesive Wear in the Mixed Lubrication Regime.* Lubricants, vol. 8, iss. 2, 2020, art. no. 16.
34. Winkler, A.; Bartz, M.; Wartzack, S. *Numerical Wear Modeling in the Mixed and Boundary Lubrication Regime.* Lubricants, vol.10, iss. 12, 2022, art. no. 334.

35. Xue Y.; Chen J.; Guo S. *Finite element simulation and experimental test of the wear behavior for self-lubricating spherical plain bearings*. Friction, vol. 6, iss. 3, 2018, pp. 297–306.
36. Рудзитис Я. А. *Контактная механика поверхностей. Часть 1.* (*Mechanics of surface contact. Part 1*). Рига: РТУ, 2007, 193 p. (in Russian).
37. Рудзитис Я. *Контактная механика поверхностей, 2-ая часть – Микротопография шероховатости поверхности (Surface contact mechanics – part 2 – Surface roughness microtopography*). Рига: РТУ, 2007, 213 стр. (In Russian).
38. Хусу А. П., Витенберг Ю. Р., Пальмов В. А. *Шероховатость поверхностей: теоретико-вероятностный подход (Surface roughness: theoretically-probabilistic approach).* Москва: Наука, 1975, 344 стр. (In Russian).
39. Buj-Corral I.; Domínguez-Fernández A.; Durán-Llucià R. *Influence of print orientation on surface roughness in fused deposition modeling (FDM) processes.* Materials, vol. 12, iss. 23, 2019, art. no. 3834.
40. Kumermanis M. *Cietu ķermeņu neregulāra rakstura virsmu 3D raupjuma parametru pētījumi. (Investigations of 3D roughness parameters of solid bodies' surfaces with irregular character).* Riga: Riga Technical University, 2012. 120 p. (In Latvian).
41. Springis G., Boiko I., Linins O. *Calculation of wear of metallic surfaces using material's fatigue model and 3D texture parameters.* Tribology in Industry, Vol. 45, Iss. 4, 2023, pp. 729–741.
42. Whitehouse, D. J.; Archard, J. F. *The properties of random surfaces of significance in their contact*. Proc. R. Soc. Lond. Ser. A. Math. Phys. Sci. 1970, vol. 316, pp.97–121.
43. Stout K. J., Sullivan P. J., Dong W. P., Mainsah E., Mathia N. T., Zahouani H. *Development of Methods for Characterization of Roughness in Three Dimensions, First edition*. London: Penton Press, 1993, 384 p.
44. Karkalos, N. E.; Thangaraj, M.; Karmiris-Obrata´nski, P. *Evaluation of the Feasibility of the Prediction of the Surface Morphologiesof AWJ-Milled Pockets by Statistical Methods Based on Multiple Roughness Indicators*. Surfaces, vol. 7, 2024, 340–357.
45. Wechsuwanmanee, P.; Lian, J.; Shen, F.; Münstermann, S. *Influence of surface roughness on cold formability in bending processes: A multiscale modelling approach with the hybrid damage mechanics model*. Int. J. Mater. Form., vol. 14, pp. 235–248.
46. Quezada, M. M.; Fernandes, C.; Montero, J.; Correia, A.; Salgado, H.; Fonseca, P. *A Different Approach to Analyzing the Surface Roughness of Prosthetic Dental Acrylic Resins*. Appl. Sci., vol. 14, iss.2, 2024, art. no. 619.
47. Hernández, H. Testing for Normality: What is the Best Method. *ForsChem Research Reports*, vol. 6, 2021, pp. 1–38.
48. *Schematic illustrations demonstrate the meaning of parameters Rsk (a) and Rku (b)* [online] [27.02.2025] Available at: https://www.researchgate.net/figure/Schematic-illustrations-demonstrate-the-meaning-of-parameters-Rsk-a-and-Rku-b_fig1_374990091.
49. Табенкин А. Н., Тарасов С. Б., Степанов С. Н. *Шероховатость, волнистость, профиль.* Международный опыт: СПб.: Изд-во Политехн, ун-та, 2007, 136 стр. (in Russian)

50. Todhunter L., Leach R., Blateyron F. *Mathematical approach to the validation of form removal surface texture software*. Surface Topography: Metrology and Properties, vol. 8, iss. 4, 2020, pp. 1–10.
51. *Leveling and form removal.* [online] [27.02.2025] Available at: https://guide.digitalsurf.com/en/guide-leveling-form-removal.html.
52. Necas D., Valtr M., Klapetek P. *How levelling and scan line corrections ruin roughness measurement and how to prevent it.* Scientific Reports , vol. 10, iss. 1, 2020, art. no. 15294.
53. Nečas, D.; Klapetek, P.; Valtr, M. *Estimation of roughness measurement bias originating from background subtraction*. Measurement science and technology, vol. 31, iss. 9 , 2020, art. no. 094010.
54. Jansons, E., Lungevics, J., Gross, K. *Surface Roughness Measure that Best Correlates to Ease of Sliding*. 15th International Scientific Conference Engineering for Rural Development: Proceedings. Vol. 15, Jelgava, Latvia, May 25–27, 2016, pp. 687– 695.
55. LVS EN ISO 25178-3:2012. *Izstrādājumu ģeometriskās specifikācijas (GPS). Virsmas īpašības: laukums. 3. daļa: Specificēšanas operatori.* (in Latvian)
56. McubeMap Ultimate 10. *The Analysis software and the Reference guide*. Digital Surf: www.digitalsurf.com.
57. Тихонов В. И. *Выбросы случайных процессов*. Москва: Наука, 1970, 392 с.

Natālija Bulaha was born in 1990 in Riga. She obtained a Professional Bachelor's degree in Mechanical and Instrumental Engineering and a qualification of Engineer in Mechanical Engineering (2012), and a Master's degree of Engineering Science in Production Engineering (2014) from Riga Technical University. Since 2011, she has been a research assistant at RTU, performing profilometric studies on surface texture and coordinating ERDF and ESF projects on heat-resistant and wear-resistant nanocoatings, as well as leading laboratory work in metrology. In parallel, she had worked as an expert in the field of welders and welding technology certification at TUV Nord Baltik Ltd, as well as a vice-chairwoman of the qualification exam in the educational program "Metalworking" in BUTS Ltd. Currently, she is a researcher at the RTU Faculty of Civil and Mechanical Engineering in the field of mechanical engineering and mechanics, studying the roughness features of various types of surfaces and their impact on wear resistance. Her scientific interests are related to computer processing of surface roughness and simulation capabilities in the finite element environment, as well as friction processes and wear mechanisms.